Functional and Structural Facts of Effective Electromagnetic Interference Shielding Materials: A Review

Jonathan Tersur Orasugh* and Suprakas Sinha Ray*

Read Online

ACCESS | Metrics & More | Article Recommendations

ABSTRACT: Electromagnetic interference (EMI) shielding effectiveness (SE) systems have received immense attention from researchers owing to the rapid development in electronics and telecommunications, which is an alarming matter in our modern society. This radiation can damage the performance of EM devices and may harmfully affect animal/human health. The harmonious utilization of magnetic alloys and conducting but nonmagnetic materials (such as carbon/graphene) is a practical approach toward EMI SE. This review is not exhaustive, although it is comprehensive and aimed at all materials for EMI SE especially graphene-based polymeric composites. It encompasses multifunctional and functional structural EMI shields. These materials comprise polymers, carbons, ceramics, metals, cement composites/nanocomposites, and hybrids. The accessibility of abundant categories of carbon-based materials in their microscale, nanoscale, and quantum forms as EMI shields as polymer−carbon, cement−carbon, ceramic−carbon, metal−carbon, and their hybrids, makes them receive much attention, as a result of their unique amalgamation of electrical, magnetic, dielectric, thermal, and/or mechanical properties. Herewith, we have discussed the principles of EMI shields along with their design and state of the art basis and material architecture along with the drawbacks in research on EMI shields.
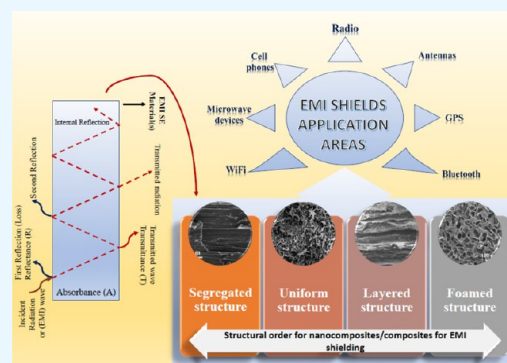
1. INTRODUCTION

The term electromagnetic interference (EMI) shielding effectiveness (SE) implies protection from microwave radiation (MW) or radio waves (RWs). For all intents and purposes, incident EMI radiation cannot infiltrate the shield, which functions as a barrier from this radiation. It is essential to distinguish EMI shielding from magnetic shielding as the latter implies shielding from a magnetic field, characteristically at low frequencies (like 60 Hz).

All electronic devices radiate/emit radio waves and microwave radiation, especially those operating within radio wave and microwave frequency ranges (like cell phones).[1−5] The apprehension is that these radiations impede electronics network and other performances owing to the metal conductor's electron's interaction with the electric field within the radiation resulting in the electronics malfunctioning. The need for more and more EMI shields from radiation sources and integrated circuit technology devices is on the rise as devices using radio- and microwaves are on the increase. For that reason, in-depth research to fabricate EMI shields has risen swiftly within recent years.[1−5]

This work presents a nonexhaustive but all-inclusive review of EMI shield research with a thorough discussion of up-to-date work in this niche, especially graphene-based materials. It also involves basic principles, categories of EMI shields or systems, applications, and drawbacks experienced and reported by researchers on EMI shields. These categories of EMI shields comprise functional, structural, and multifunctional shields.

Systems in the form of polymers, ceramics, carbons, metals, cements, their composites, and hybrids are structural materials that display SE. Currently, composites and noncomposite materials are reportedly broadly investigated and are extremely suitable in EMI shielding products. With consideration of publications on Science Direct (which was searched for "Effective electromagnetic interference shielding material") for the last 20 years of data on composites and noncomposite materials for EMI shielding as depicted in Figure 1, there is an increased demand for materials in this niche year-by-year in several fields of research including Materials Science (3,603), Engineering (2,110), Physics and Astronomy (1,475), Chemistry (931), Energy "E" (797), Chemical Engineering (577), Medicine and Dentistry (367), Environmental Science (338), Earth and Planetary Sciences (304), Computer Science (277), etc. Despite the massive range of literature on the EMI shielding
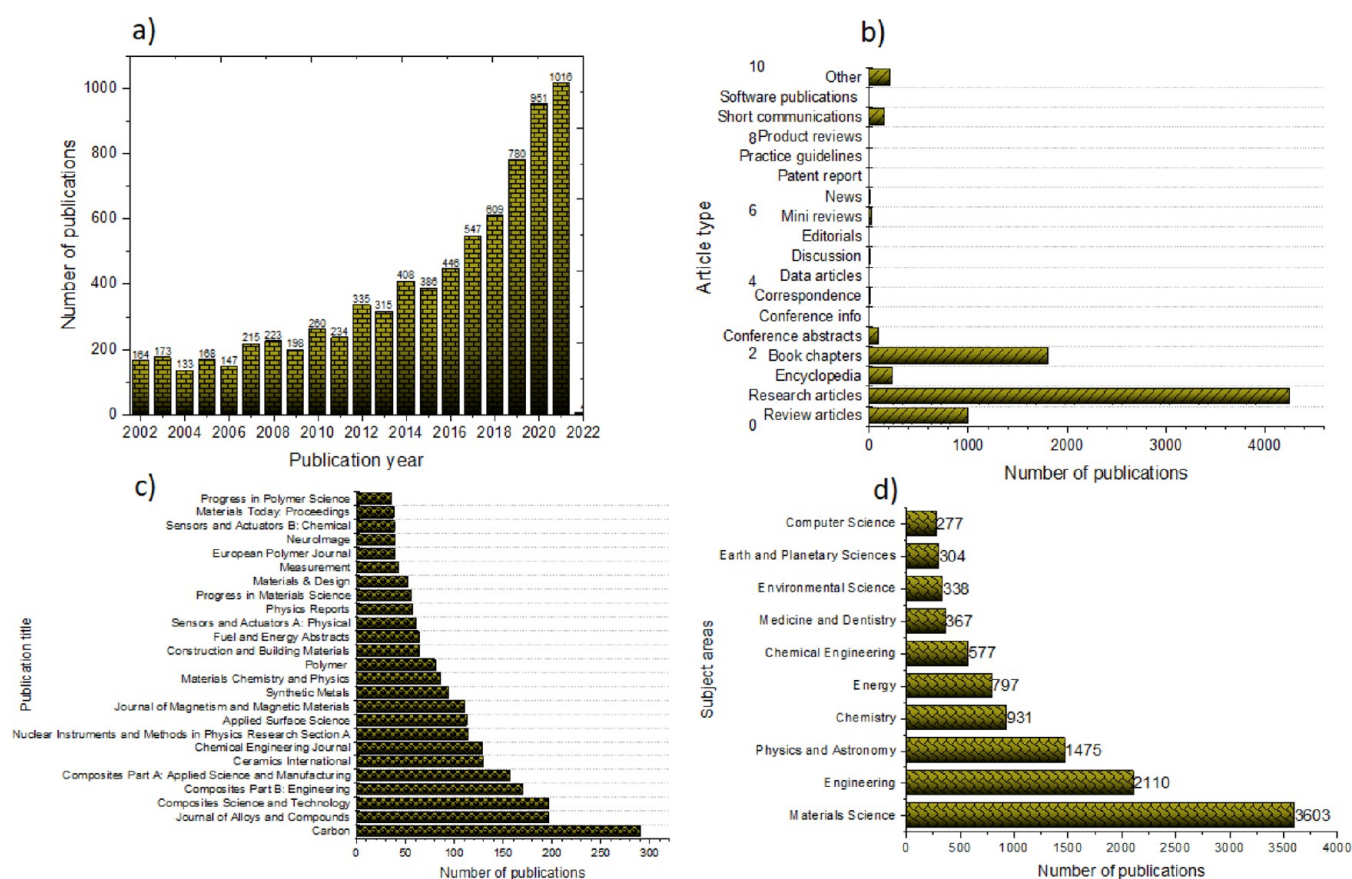
Figure 1. Publication database on Science Direct for the last 20 years (22/07/2021) for composite and noncomposite materials for EMI shielding: (a) number of publications per year, (b) number of publications with respect to article/publication type, (c) number of publications per title/publisher, and (d) number of publications with regards to the subject area.

character of diverse systems, a scientific study of the magnetic and conductivity performance along with the precise surface/interface space on the SE at numerous combinations of frequency and temperature is brutally insufficient.

2. FUNDAMENTAL PRINCIPLES

The radio wave (RW) region includes frequencies extending to or beyond 10^4 to 10^{10} Hz (which implies wavelengths 10^1 to 10^4 m). The microwave (MW) region comprises frequencies ranging between 10^9 and 10^{12} Hz (which suggests wavelengths ranging from 10^3 to 10^0 m). These two (radio wave and microwave) regions overlap where the vital frequencies exist within the GHz range. For instance, 1 GHz frequency matches 0.30 m wavelength giving rise to long wavelengths.[3,6,7] This is the reason that EMI shields could be a mesh made of metal wires or sheet form having openings large enough for someone to see through, such as a microwave oven door. Owing to the long wavelengths, EMI shields should be premeditatedly fabricated considering the macroscopic structure, even though most researchers working on EMI shields have concentrated on these materials' micro- and nanostructural aspects.[6]

EMI shields encompass mainly absorption and/or reflection of the electromagnetic radiated waves, as schematically shown in Figure 2. The reflection of EM waves results in the bouncing of the radiation off from the walls of the EMI shield.[3] The radiation reflected may be detrimental to the environment, chiefly to the living organisms present, making the absorption mechanism preferable for SE materials considering the safety viewpoint.[3] For low visibility (stealth), a reflection of EM radiation is also
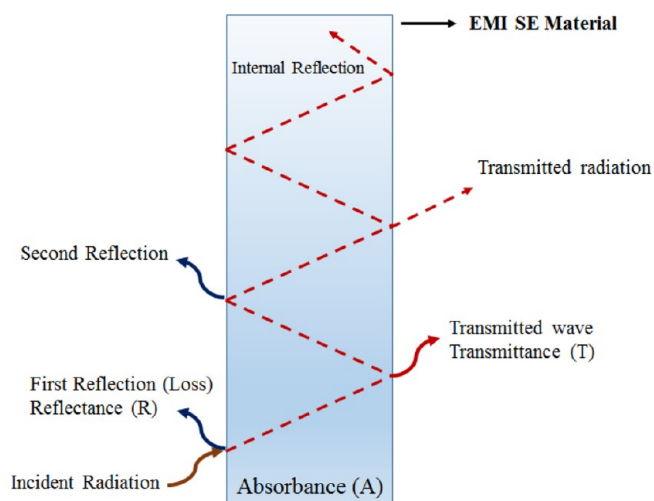

Figure 2. Scheme representing EMI SE mechanism of a predetermined material.

undesired, particularly considering the fact that the reflected radiation may reach the radar, hence making the material/system detected.

Decreasing the electric resistance pair between the fabric and the close medium is a good technique for reducing reflection. Though EMI shields are typically conductive fabrics (e.g., metals, carbons, their composites, their hybrids, etc.), the electric resistance pair has a substantial tendency to influence the

conductivity of the fabric(s): the material's nanostructuring via layering within the nanometer scale presents an opportunity to fabricate novel materials having reduced reflection.[8]

Power loss refers to the loss of power thanks to the interface between an incident radiation source and the shield. This includes the loss of electrical power and, consequently, the loss of magnetic power (MPL). The electrical/magnetic character of the constructed shield determines the relative importance of the two types of power loss. As an illustration, the MPL is important for a magnetic EMI shield but irrelevant for a nonmagnetic one. The relative amplitudes of the electrical field and the field within the source radiation both play a role in the relative importance of these two kinds of power loss.

The power loss owing to the shielding is presented in decibels (dB) and is mentioned as the SE or total SE (SE_T).[9] Some portion of this loss as a result of absorption is understood as the absorption loss (SE_A). The portion of the loss as a result of reflection is referred to as reflection loss (SE_R). Mathematically, the quantities are outlined in eqs 1−3.

The scattering factors (S-parameters) define the response of the network with N anchorages to signal(s) occurrence to 1 or many ports. Within the abbreviation referring to S-parameters, the primary range within the subscript indicates the returning port, whereas the second range indicates the incident port. The abbreviation S_{21} denotes response at port two ensuing from proof at harbor one.

The quantities SE_T, SE_R, and SE_A are derived from S-parameters via the equations[6]

$$SE_T = -10 \log(T) = -10 \log |S_{21}|^2 \tag{1}$$

$$SE_R = -10 \log(1 - R) = -10 \log(1 - |S_{11}|^2) \tag{2}$$

$$SE_A = SE_T - SE_R - SE_M \tag{3}$$

Here, T represents the constant of transmission/coefficient, referring to the portion of input power entering the interior of the sample, while R is the reflection coefficient, representing the portion of input power that is mirrored from the surface of the sample. Each T and R ought to be represented as fractions/percentages and will not be reportable within the dB. SE_M (eq 3) signifies the shielding arising from manifold reflections within the interior portion of the sample.

In actual instances, SE_M is every often so insignificant, if the overall shielding (SE_T) exceeds 15 dB. In this case, eq 3 becomes[6]

$$SE_A = SE_T - SE_R - 10 \log(T/(1 - R)) \tag{4}$$

The influence of absorption (A) denotes the magnitude relation of SE_A to SE_T. The SE_A will increase with growing frequency, as specified by magnetism theory:[6]

$$SE_A = 131.4t \sqrt{\mu_r \sigma_r f} = 131.4t \sqrt{f\mu\sigma/(\mu_0 \sigma_{Cu})}$$
$$= 8.68t \sqrt{\pi f \mu \sigma} \tag{5}$$

Here, t denotes sample thickness in meters, f represents the frequency within the cycle, μ_r stands for relative magnetic permeability with Cu as reference material, σ_r denotes EC with Cu as reference material, σ is the electrical conductivity (EC), and μ is the magnetic permeability, $\mu = \mu_0 \mu_r$, $\mu_0 = 4\pi \times 10^{-7}$ H/m. Equation 5 signifies a conductive system. It signifies that SE_A increases with rising frequency if μ_r and σ_r do not decrease. It conjointly suggests that SE_A at a given frequency will increase with each permeability and conduction. The EC and magnetic

permeability (MP) values for conventionally known materials are presented in Table 1.

Table 1. EC (Ω^{-1} m^{-1}) and MP (H/M) of Conventional Materials with Respect to Cu

samples	EC (Ω^{-1} m^{-1})	MP (H/M)	ref
Cu	1.0	1.0	10
Au	0.7	50−1000	10
Ag	1.05	1	10
carbon fiber	2.75×10^{-2}	0.97	11
graphene	0.1	1.01	11
CNTs	0.1	1.01	11
graphite	1.83×10^{-2}	0.99	11
Fe	0.17	50−1000	10
Al	0.1	1	10
Ni	0.2	1	10

Understanding the relationship between an EMI shield with magnetic and electrical fields within the EM field is vital for its effective fabrication toward efficient EMI SE. The magnetic property of the material promotes EM wave absorption because of the interface of the shield's magnetic dipoles with the flux within the field zone. The relevant features of the shields' magnetic allure include the dipole friction (that increases with rising frequency and relies upon the magnetic domains and/or domain boundary quality dimensions), dipole−dipole interface, magnetic susceptibleness, and magnetic links.[12] The electrical polarizability of EMI shields additionally boosts the absorption because of the electrical dipoles' interaction within the material and/or with the electrical field within the EM field zone. The relevant features of the material character include the electrical dipole friction (that increases with increasing frequency), dipole−dipole interface, matter property, and electrical suscept-ibleness.[12]

The material characteristics relate to its conductivity behavior via the Kramers−Kronig correlation.[6] For instance, among graphene-based systems fabricated through heat treatment at diverse temperatures, the conduction and the real and imaginary components of the permittivity are all enhanced with increasing temperature of heat treatment.[6]

The conductivity property conjointly contributes to the EMI SE energy loss, signifying the imaginary part of (complex number, pure imaginary number) complex permittivity. Among EMI SE materials that do not seem to be magnetic, high conduction is often well-thought-out within the trade as the primary attribute for getting high SE. This stress on the conduction is partially a result of the benefit of the activity of the shield conductivity. Nevertheless, high conduction is not essentially the first condition for EMI SE of the shields among nonmagnetic systems. There are SE alternative factors, such as mentioned below. One issue relates to the space/area/expanse/extent of the shields or the interfacial area within the EMI shield. Due to the skin-effect, a large specific surface or interfacial area increases the specimen part of that network's degree of EM radiation absorption and so improves the SE.[13] The skin effect is a propensity for alternating current (AC) to flow mostly toward the outside surface of an electrical conductor, such as a metal wire. Skin effect and skin depth describe the behavior of EM waves inside conductive metals and have an impact on the design of EMI shields.[13] The interfacial interaction signifies the shielding part (for instance, the reinforcing active filler or the polymeric matrix in some cases) and the nonshielding part (for

instance, the polymer matrix) used to fabricate the shield. Its nonshielding part is comparatively clear to the EM wave as a result of a reduced extent of interface within the field.[6] With regard to a particular porosity for an exceedingly porous shield, a more modest component size of the permeable microstructure offers a superior explicit span and, subsequently, more prominent SE.[3,6] A smaller component size of the reinforcing filler affords superior explicit interfacial space in relation to a set filler volume fraction in an extensively designed polymeric composite material, hence enhancing shielding. This may account for some of the use of nanofillers and SE enhancers in composites used to create EMI shields.[6]

One more issue correlates with the electrical property that fosters the EMI shielding, owing to the networked connection of the electrical field paths within the shield. This continuity conjointly permits the flow of eddy current induced by the field of force, thereby encouraging MPL. Consequently, electrical percolation in a novel polymer composite with a semiconducting reinforcement and a nonconductive polymeric matrix is gainful for EMI shield performance. The reinforcing filler percolation threshold is at a low level once the reinforcing filler aspect ratio is high. Nanofibers (NFs) present a better ratio in this regard when compared to their counterparts (microfibers), which is another factor for the adoption of NFs over MFs by researchers.[6]

Considering a magnetic EMI shield, the magnetic stability of the magnetic part is required due to the field of force lines which should be continuous for effective SE.[3] Hence, the EMI shield's reinforcing filler's (magnetic/nonmagnetic) magnetic percolation in a fabricated composite material is vital for effective SE.[3]

The magnetic material and conductivity behavior along with its specific interfacial area contribute to regulating the SE. What is more, we know that every behavior of the EMI shield hinges upon the temperature and/or frequency of application. The results of the frequency and temperature do not seem to be solely related to application; however, they shed light on the mechanisms of the material's shielding performance. It is attainable that, for a specified EMI shield, the predominant shielding mechanism hinges upon the mix of its temperature and frequency. Despite the massive range of publications related to the EMI shielding performance of diverse fabricated shields, a scientific study of the results of the magnetic and conductivity behavior and the specific surface/interfacial area upon the SE at numerous combinations of temperature and frequency is terribly scarce. Table 2 presents examples of a restricted style of such a scientific study. The result of the frequency has attracted and been given far more attention compared to the temperature

result. Previous work has emphasized EMI materials formulations toward enhanced SE, although not sufficient consideration to the scientific know-how for these materials' improvement.[6]

The dependence on frequency tends to be significantly vital at frequencies around specific absorption mechanism deviations (like an amendment from coupled polarization at low frequencies toward electronic polarization at elevated frequencies). Ceramic materials incline toward their own tougher frequency dependence relative to graphene/carbon-based materials and metals owing to the partly ionic character of ceramic materials and the slowness of ionic motion in comparison to its electronic motion within the structure.[6] For emblematic sensible applications, a consequential disparity of the shielding due to frequency is not wanted. Attaining high SE over a large frequency range may be a common goal in the thorough analysis of graphene-based polymeric composite materials for EMI shielding.[3] This property has been studied and reported as depicted in Figure 3.

Diminished reflection is appealing from the protection vantage point. Magnetic particles having conducting properties tend to reflect considerably owing to their excessive impedance disparity. Hence, fabricated magnetic substances having low conductivity are favored for decreasing the incident wave reflection. Correspondingly, dielectric (polarizable) substances having conductive properties have a tendency to reflect significantly. Though reflection is significant, absorption is even additionally vital. Thus, it is necessary to determine both the SE_R and SE_A for the comprehension of the shielding phenomenon. EM radiation absorption leads to heating, that is, the translation of the EM E into thermal E, which consequently affects the extent of reflection and absorption. By increasing the absorption within the acceptable temperature range, the EMI shielding is enhanced, as reported for graphene.[1]

3. CATEGORIES OF EMI SHIELDS

Materials used for the fabrication of EMI shields include carbons, ceramics, cement, metals, conducting polymers, related nanocomposites/composites, etc. These nanocomposites/composites (amalgamations of materials) represent the most utilized materials for the fabrication of EMI shields.

Graphene/carbon-based materials and metals dominate because of their high conduction and also the related availableness of itinerant electrons for interacting with the electrical field within the radiation. Ceramics or cement-based materials are not as effective; however, the functional groups within them will respond to the electrical field within the region of radiation. Polymeric matrices are even less successful, except if they are a conductive type. For these materials, the presence of magnetic constituents improves the EM wave shielding because of the collaboration of the magnetic component with the magnetic field within the radiation zone. The functional and multifunctional EMI SE shields and their fabrication in a very cost-efficient fashion with the scale and form needed are critical. Composite/nanocomposite shields offer an efficient avenue for achieving the fabrication of the aforementioned/desired EMI SE materials.[3,6] These composite/nanocomposite materials are principally polymeric matrices and/or cement-based matrix composites which involve abundantly cheaper manufacturing cost than their carbon-matrix, ceramic-matrix, or metal-matrix counterparts. A method neglecting hybrids/composite systems encompasses the compaction of predetermined particles that may interlock automatically to themselves. An instance is the

Table 2. EMI SE Correlation with Electrical, Magnetic, and Structural Traits[a]

| feature	Ni NFs	Ni fibers A	Ni fibers B
diameter (μm)	0.4	2	20
EMI SE (1−2 GHz),19 vol % reinforcing filler	92	72	5
magnetic hysteresis E loss, for the nickel part of the composite (J/m^3)	7370	4930	1020
magnetic coercive field (kA/m)	16.9	4.7	0.5
resistivity (DC), 19 vol % filler in composite (Ω·cm)	1.5×10^{-3}	2.9×10^{-4}	5.3×10^{-2}
grain sizes (μm)	0.016	0.018	2
number of grains per diameter	9	110	10

[a]Information derived from refs 14 and 15.
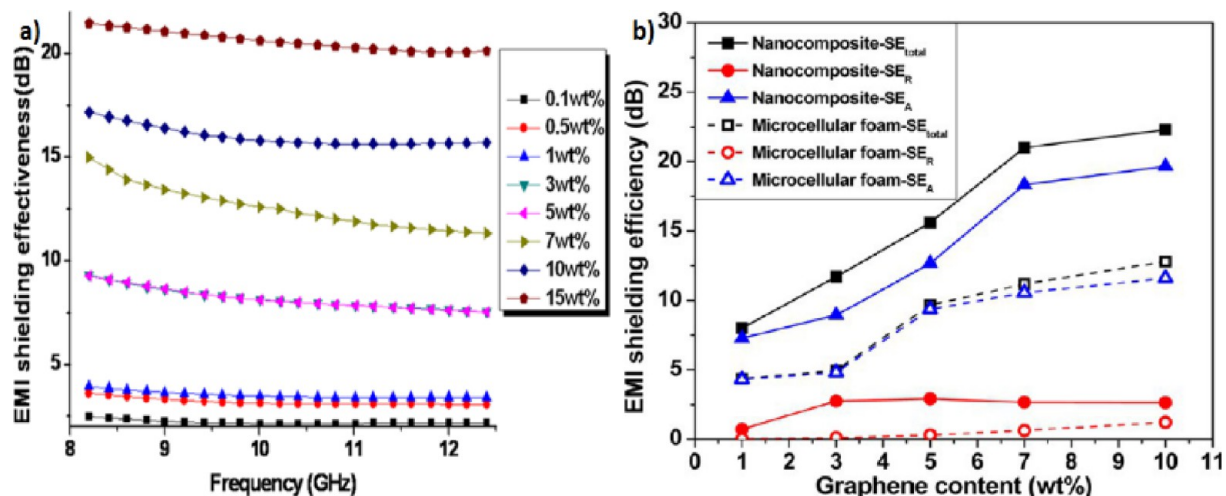
Figure 3. (a) EMI SE of graphene/epoxy composites with various solution-processable functionalized graphene (SPFG) loadings as a function of frequency in the X-band. Reproduced with permission from ref 16. Copyright 2009 Elsevier Science Ltd. (b) SE_T, SE_R, and SE_A of PEI/graphene nanocomposite and microcellular foams at 9.6 GHz. Reproduced with permission from ref 17. Copyright 2013 American Chemical Society.

exfoliation of graphite followed by its compression in the absence of a matrix/binder resulting in a film/sheet.

3.1. Functional EMI Shields Versus Structural Shields. EMI shielding materials are categorized as either structural or functional materials. Functional shielding materials (i.e., non-structural shielding materials) are very vital in this niche. EMI functional shielding materials are frequently utilized as a shielding component within devices like mobile phones, where they are merged/added in or upon a given structure. In most cases, research patterning EMI shields focuses more on functional shields instead of their structural counterparts.

The structural materials have to do with materials that also perform the load-bearing role of a structure. For instance, continuous-carbon fiber polymeric-matrix nanocomposites/composites are applied in lightweight structures, such as frames, with consideration to the physical science in which shielding is required. One more example is that of cement-based structural shields, which are vital for civil engineering infrastructure, such as a concrete cowl of a large transformer dome. Shielding is additionally required for buildings to evade EM forms of spying and to offer EMP (electromagnetic pulse) shielding. Structural EMI shields (like graphene-based composites) usually are multifunctional. In comparison to incorporating functional shields in/on a given structure so as to achieve a structure proficient enough for the intended shielding, multifunctional structural EMI shields are drawing researchers' attention owing to their high durability, low-cost, and high functional surface area (large functional volume) along with enhancement in mechanical performance. Considering the restricted volume of a device like a mobile phone, functional EMI shields have to be compelled to be effectual even at low thickness.

Moreover, in order to reduce the mass of the device, functional EMI shields with low density are fascinating. Nevertheless, being effectual even at low overall material density is not important in the actual application unless there's extra effectiveness even at low thicknesses. Conversely, because of the large size of infrastructures, multifunctional EMI shielding materials do not have to be compelled to be effective at low thicknesses. Moreover, except for lightweight structures like airplanes, multifunctional EMI shielding materials do not have to be mandated for effectual performance at low density. Mainly,

low density is not typically required for civil engineering structures where cement-based shields are foremost.

3.1.1. Metal-Based EMI Shields. For a long time, metals in their bulk form and/or glaze forms have been utilized for shielding EM waves. The only typical instance of bulk kind of metal is film Al custom created electronic enclosures. In the instance of metals in coatings, a typical instance is electroplated Ni on electronic components that require shielding from EMI, as Ni is conductive as well as ferromagnetic. These coatings face the challenge of being scratched even though the scratches, to some extent, tend to be tolerable as a result of the long radiation wavelength.[6] The majority of these materials are faced with the challenge of their large mass and volume. Additionally, the enclosures are challenged by EMI shielding deficit at the joints/seams at intervals inside the enclosure, for instance, the joint on an EMI shielded room door, where EMI gaskets are used to eliminate this challenge. EMI gaskets must be robust (springy), additionally, to being an effective EMI shield.[6] Metals/alloys possessing magnetic properties are outstanding for EMI shielding via absorption. Magnetic alloys such as permalloy (Ni (80 wt %)−Fe (20 wt %) alloy having comparative MP of 20000 (at 1 kHz)), mu-metal (Ni−Fe ferromagnetic alloy: comparative MP of 100000 (at 1 kHz)), along with stainless steel (#430, ferritic, having comparative MP 500) are some of the instances in this niche, though these alloys possess large weight/mass, owing to their high densities. Nickel presents itself as a magnetic metal also, but the relative permeability being 100 is somewhat low.[9] Nevertheless, it is attention-grabbing to researchers and industrialists considering its ease of coating onto predetermined surfaces via electroplating.

The harmonious utilization of magnetic alloys and conducting but nonmagnetic materials (such as carbon) is a practical approach toward EMI SE. For instance, magnetic alloys like FeNi micro/nanoparticle CNTs are more effective than magnetic alloys as particles unaccompanied or CNTs unaided as active reinforcement in the polymeric-matrix nanocomposite.[18] Also, a mu-metal magnetic alloy and graphite flakes have been reportedly utilized as a blend in EMI shielding material. By utilizing a much lower magnetic constituent compared to the conductive constituent in a polymeric-matrix composite, the EMI SE is higher than that of the composite possessing the
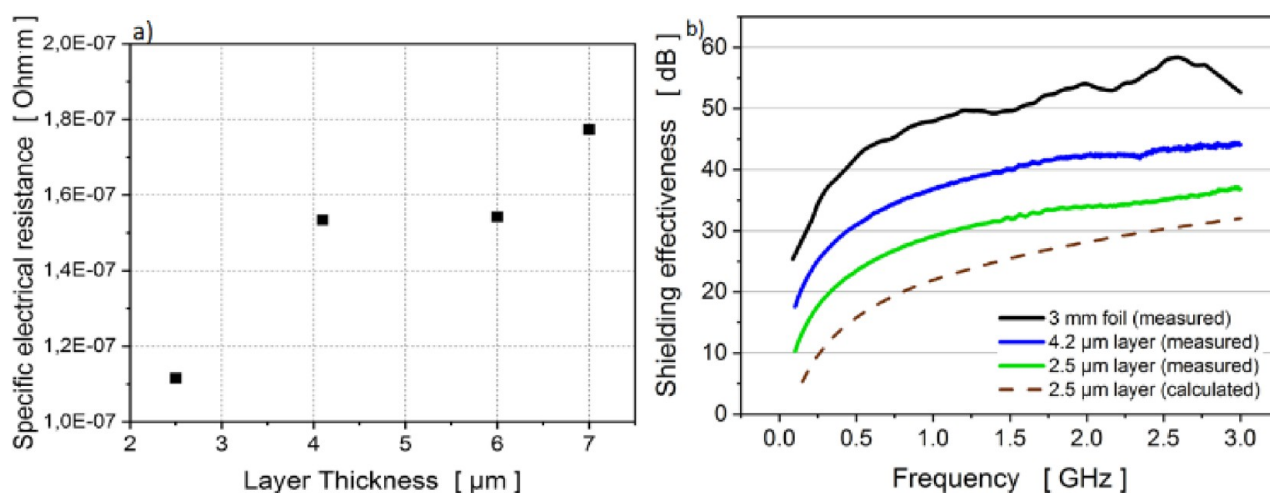
Figure 4. (a) Specific electrical resistance as a function of layer thickness. (b) Shielding effectiveness in magnetic near field configuration as a function of frequency for an aluminum foil (smoothed) and two aluminum layers of different thickness. The reference dashed line was calculated according to the impedance concept (used parameters: source/sample distance = 0.25 mm, aluminum layer thickness = 2.5 μm, electrical conductivity = 7.106 S/m). Reproduced with permission from ref 21. Copyright 2020 Elsevier Science Ltd.

magnetic constituent alone or the conductive constituent solely as the reinforcement.[19] The magnetic constituent of the material is effective toward enhanced EMI shielding as long as the composite electrical resistivity is <10 Ω cm.[5]

A broadly acknowledged notion is that EMI shields having high conductivity provide a status quo where the SE is principally reliant on reflection instead of absorption.[3,5,6,8] High conductivity, however, may be connected to the SE being predominantly caused by absorption, as discussed in the following paragraph with respect to Al; thus this idea is not necessarily true;[20] Al is known to be the foremost metal used in EMI materials with good SE. In order to comprehend the features/factors governing the EMI shielding of these materials, it is significant to compare the SE of these materials with their nano/microstructural parameters, magnetic, electrical, and dimensional characteristics/properties.[3−6] This relationship has been studied for nickel, which is conductive and ferromagnetic. The SE, magnetic properties,[14] electrical resistivity,[14] and nano/microstructure[14] are presented in Table 2 for fibrous nickel having three diverse diameters of 20, 2, and 0.4 μm. The 0.4 μm fibrous Ni diameter is Ni-glazed CNFs, where the carbon core diameter is ∼0.1 μm. At similar filler weight content (19 vol %) and similar nonconductive poly(ether sulfone) polymeric-matrix, the EMI SE at 1−2 GHz, hysteresis energy loss, and coercive force wholly decline unchangingly with increasing diameter of Ni. Nevertheless, the DC resistivity is the lowermost around 2 μm diameter, due to the two contending influences, (i) reduced resistivity via improved contact of the Ni filament units, empowered by a lower cross-section (larger aspect ratio) and/or (ii) increased resistivity via the presence of a higher number of touch points, due to reduced diameter. Hence, a concession among the two influences, as revealed by the transitional thickness, presents the smallest possible resistivity.

The 0.016 and 0.018 μm grain size is analogous for the widths of 0.4 and 2 μm but higher for the 20 μm diameter. The number of grains per unit or grain size does not correlate with the diameter and/or resistivity. The relative findings in Table 2 disclose that higher EMI SE relates to higher hysteresis E loss along with the coercive force values and minimal diameter. Still, the SE does not relate to their resistivity or grain size, along with

the number of grains per unit diameter. At a similar filler concentration, a small diameter correlates to a higher specific interfacial area; owing to skin-effect, SE is enhanced by a higher specific interfacial area. Skin-effect impacts and governs the conductivity effect toward regulating the shield's SE.

In the same way, the energy loss due to hysteresis and coercive force is enhanced by a higher specific interfacial area; as absorption takes place within the shield's interior, the contribution from absorption is increased with increasing material thickness.[1] Likewise, higher conductivity produces a significant mismatch in impedance between air and the specimen, thus resulting in significant incident EM radiation reflection. Aluminum EMI shields have been reported to be significantly dominated by the absorption mechanism,[15] where the SE_R is lower than SE_A; for instance, at 1 GHz, SE_A was 43 dB, whereas the SE_R was reported to be 5 dB.

The dominance of absorption occurs notwithstanding the high conductivity coupled with the lower thickness of aluminum foil applied. The domination is partially ascribed to the higher value of the comparative electric permittivity of 54,800 at a frequency of 2 kHz.[12] The resultant higher permittivity is a result of a small portion of free e− within the Al atoms, while the permittivity-aided polarization enhances the absorption. Recently, a group of researchers synthesized a 12% Al-doped MoS_2/rGO nanohybrid by a facile and highly responsive hydrothermal technique. The nanohybrid showed high AC electrical conductivity and EMI SE values.[14] Also, a 3D porous nickel metal foam/polyaniline heterostructure having outstanding EMI SE and absorption based on the predetermined construction of its macroscopic conductive network has been reported.[21] Heinß and Fietzke[21] have shown in their work that the thickness of the layered composite EMI shield and specific electrical resistance increased with the increasing thickness of the samples, as shown in Figure 4.

3.1.2. Carbons. Carbon materials (such as graphene, graphite, coke, carbon nanofibers (CNFs), carbon fibers (CFs), and carbon nanotubes (CNTs)) do not seem to be solely conductive electrically; they are smart EM absorbers over a broad frequency.[6,22−24] Differing kinds of carbon vary greatly in conduction, structure, morphology, and price challenges as premised by some researchers.[6] CNFs (mentioned above) have
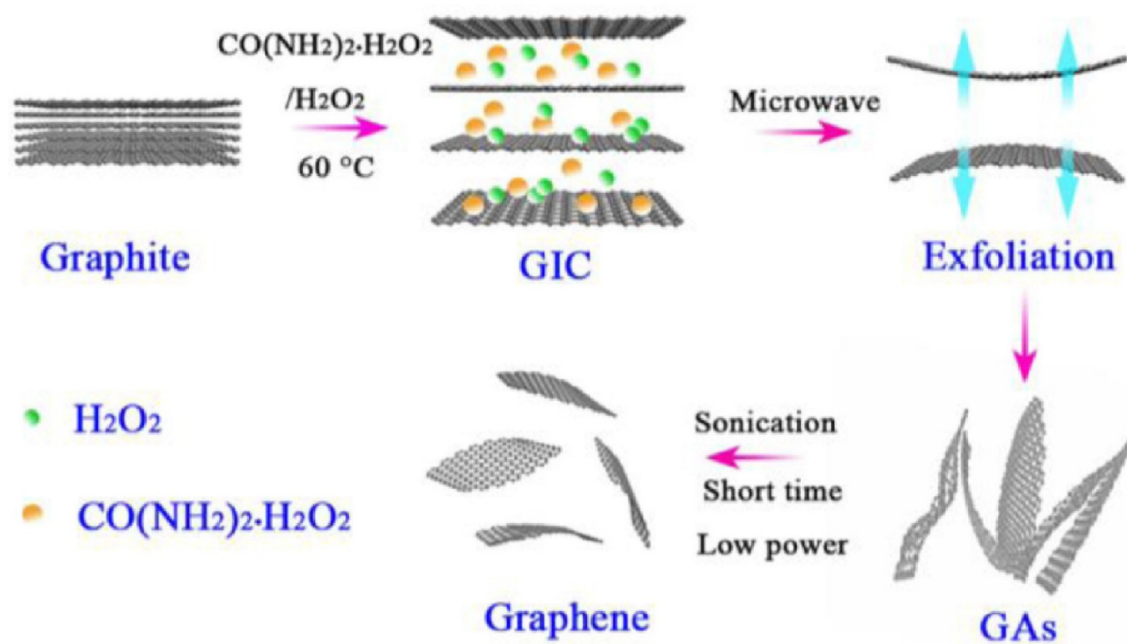
Figure 5. Schematic of the intercalation and exfoliation of graphite to graphene via the optimized route. Reproduced with copyright permission from ref 26. Copyright 1996 Springer.

originally also been referred to as C-filament. A principally striking category of graphitic material referred to as exfoliated graphite, as typically shown in Figure 5, is obtainable through intercalation of graphite flakes, followed by swift heating (direct or indirect), which resulted in graphite exfoliation.[25,26] Every single piece of exfoliated C is wormlike, owing to the severe enlargement along the c-axis and the succeeding length in the same path.[6,25] Mechanical interlockings took place as the worm-like materials were compressed among the neighboring worms, resulting in a sheet without the inclusion of a polymeric matrix. Owing to the sheet's flexibility, it was denoted as "flexible graphite". As a result of its high extent of compression throughout the preparation of the versatile C, the sheet exhibited robust crystallographic most favored positioning of the carbon layers within the sheet axis. Owing to the prevalent orientation, these sheets are very anisotropic, having an electrical conductivity profusely higher within the sheet axial plane compared to the perpendicular direction.

Additionally, the method of exfoliation leads to a degree of open porosity along with blocked pores within its structure, leading to an enhanced surface area. Higher surface area is desired for enhanced EMI shielding, due to skin-effect: looking at these factors, flexible graphite displays EMI SE of ~130 dB,[27] being the higher threshold of the power loss measurement. What is more, because of the cellular structure and most favorable alignment, the sheet is robust along the path perpendicular to the sheets' plane; the resiliency permits versatile C to function as an associate EMI seal. Further lures of exfoliated flexible graphite are high thermal conductivity and chemical inertness along with low thermal expansion coefficient, all principally treasured in microelectronics fabrication. Regarding versatile C, SE_T and SE_A are enhanced with the progressive increase in frequency; specified SE_T exceeding 49 dB and SE_A exceeding 44 dB are obtainable. The frequency dependency is weak for each SE_A and SE_R. The SE_A is far bigger than SE_R, indicating the absorption influence increasing with cumulative frequency.[15] Due to the cellular structure, there is a hefty body in versatile C, as its

density is high in the case of ideal C. The thickness of carbon denotes its thickness arising from the carbon itself, the specimens' portion excluding its pores. The SE_A relative to the unit thickness of the specimen will increase with rising frequency, with its value compared to the thickness of carbon that is close to the specimen thickness.[18] It demonstrates how vital the consideration of the body within the shielding material is.

The SE_A relative to unit thickness is far lower for versatile C than Al.[15] This is often partially because the Al is far less thick than the versatile C. Moreover, both conduction and permittivity of versatile C are measured lower than those of Al.[6] Carbon activation encompasses the reaction (chemical) resulting in its surface evolved porosity. Because of the higher surface area along with the skin-effect, CFs (activated) are simpler as shielding material compared to unactivated carbon.[6] This activation process reduces the carbon fibers' mechanical properties; precisely, the decrease is additionally substantial for a higher extent of activation. Hence, its activation ought to be light for instances where the carbon fiber is aimed at structural application. However, if the fiber is not for structural utilization, the activation extent does not have to be restricted. Partly because of the higher surface area along with their skin-effect, nanocarbons (nCs) especially graphene, CNFs, and fullerene are considered effective as reinforcing fillers in EMI shields. Rather than dispersing the nC in an exceedingly bound matrix, it is possible to create nC paper (like fullerene paper), as reinforcing fillers in nanocomposite systems.[28]

Hybrid nCs and porous nCs are chiefly synthesized for EMI shielding by augmenting their surface area and reducing impedance mismatch among the shield and the surrounding air. Reduction in the impedance mismatch aids the reduction of the SE_R, boosting the absorption loss, a primary essential mechanism for shielding in carbons. The amalgamation of continuous CFs and fullerene has drawn great attention because the nanotubes are aligned on the axis of the CF.[29] These hybrids shields may be made of carbons and/or metals as active fillers,
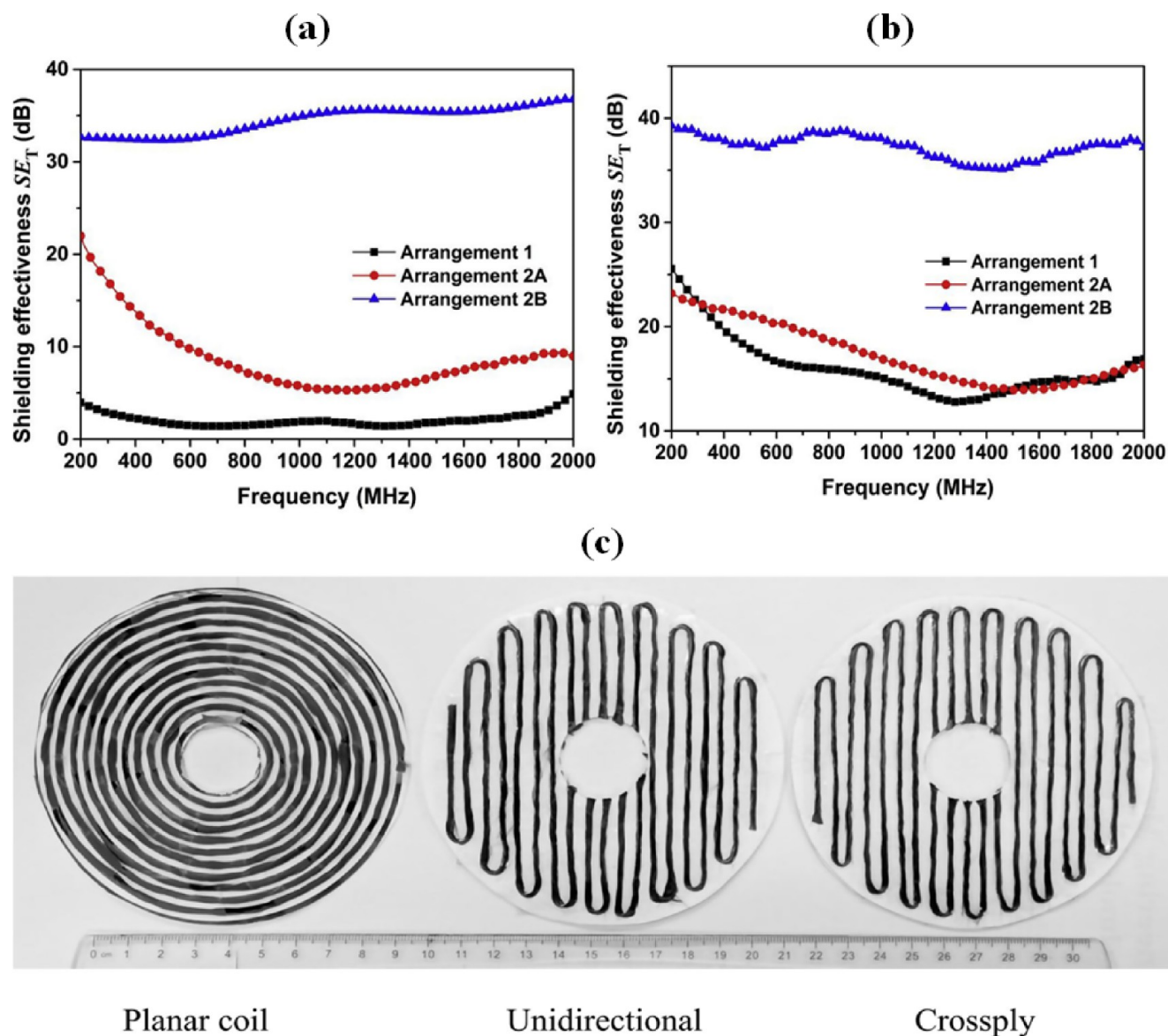
Figure 6. (a) Absorption loss of continuous carbon fiber (uncoated) with three fiber chain planar arrangements. (b) Absorption loss of continuous carbon fiber (nickel-coated) with three fiber chain planar arrangements. (c) Optical photograph of the specimens corresponding to the 3 platelike arrangements, together with a ruler with major divisions in centimeters. The backside of the cross-ply arrangement is hidden from the reading in panel c, such that the photos seem to be identical for the cross-ply (Arrangement 2B) and unidirectional (Arrangement 2A) arrangements in panel c. Reproduced with permission from ref 32. Copyright 2019 Elsevier Science Ltd.

whereas an associated instance may be a hybrid made of CFs, Ni nanoparticles, and graphene.[30] For polymeric matrices that are primarily clear to radiation, a NF reinforced composite presents superior properties to its microfiber (MF) counterpart in EM wave shielding. Once the NFs and MFs are taken at an equal volume fraction, a phenomenon often due to the skin-effect along with higher interfacial interaction within the NF-reinforced composite occurs. Metal-glazed CF has been reported to be more efficient in EMI shielding compared to unglazed CF.[14] Owing to the skin-effect, metal-glazed nC like nickel-glazed CNFs (referred to as Ni-glazed C-filament, or Ni-filament) are measured even easier.[14,15] Nickel coating of CF/C provides higher conductivity and magnetic behavior in comparison to uncoated CF. The application of nickel-coated CF as a functional reinforcement in a matrix resulted in a composited EMI shield that exhibited SE of 87 dB (1−2 GHz) at a filler volume fraction of 7 vol %.[14,15] In EMI seals/gaskets, the

volume fraction of the filler should be continuous/unbroken and low, as resiliency arises from the polymer matrix and it decreases with an increase in filler content;[31] hence, in EMI seals, the reinforcing filler is expected to be effectual at even low volume fraction.

Continuous CF polymer matrix and/or carbon matrix (nano)composites have been proven to possess extremely excellent SE. The latter is additionally called carbon−carbon (C−C) (nano)composites. In this kind of material, SE is partially because of the CF continuity in the composites. Though electrical conductivity continuity is effective, even at high frequencies, the amplitude of the charges is not massive. Because of the carbon matrix's physical phenomenon and the nonconductive nature of the compound matrix, the C-matrix composite seems to be more practical compared to its polymer matrix counterpart for EM wave shielding.[32] The C-matrix boosts the electrical continuity, which additionally contributes

Table 3. EMI SE Properties of Graphene Polymer Composites within the X-Band Frequency Region

nature of polymers	composite thickness	nature of graphene	concentration/loading of graphene	preparation technique	EMI SE (dB)	ref
PVC	1.80 mm	graphene	5 wt %	solution intercalation—solvent casting	13.0	35
PVDF		graphene	7 wt %	in situ polymerization	28.0	36
PEI	2.30 mm	graphene	10 wt %	in situ intercalation—solvent casting	11.0	17
PU	20.00 mm	rGO	3 mg/mL	dip-coating	12.4	37
PU	2.00 mm	graphene	7.7 wt %	solution mixing—solvent casting	35.0	38
PEDOT—PSS	1.15 mm	graphene	58% weight fraction	chemical vapor deposition (CVD)	91.9	39
PMMA	0.79 mm	graphene	5.0 wt %	solution blending—melt compounding—batch foaming process	19.0	40
PMMA	3.40 mm	graphene	4.23 vol %	batch foaming process	30.0	41
PS	2.80 mm	graphene	10.0 wt %	compression molding	18.0	42
PS	2.50 mm	graphene	7.0 wt %	high-pressure solid-phase compression molding	45.1	43
Epoxy		rGO	15.0 wt %	in situ intercalation—solvent casting	21.0	16
Epoxy	3 mm	GNPs/rGO	20.0 wt %	in situ intercalation—solvent casting—templating method	51.0	44
PDMS	1.00 mm	graphene	0.8 wt %	template-directed chemical vapor deposition (CVD)	30.0	45
Polyimide (PI)	0.80 mm	rGO	16.0 wt %	solvent casting via in situ polymerization	17.0—21.0	46
UHMWPE	2.50 mm	rGO	0.66 vol %	melt compounding/hot press	28.3—32.4	47
PVDF	2.00 mm	graphene	15.0 wt %	water vapor induced phase separation	45.6	48
PS	2.50 mm	graphene	30.0 wt %	high-pressure compression molding plus salt leaching	64.4	49
PMMA	2.00 mm	graphene	20.0 wt %	solvent casting	21.0	50
PVC	2.00 mm	graphene	20.0 wt %	solvent casting	31.0	50
PPY		graphene	5.00 wt %	in situ polymerization	53.0	51
PPY	2.50 mm	rGO		in situ polymerization	48.0	52
PANI	5.00 μm	graphene	1.00 wt %	in situ polymerization—solution intercalation—casting	32.0—42.0	53
PANI	2.00—7.00 mm	GO	25 wt %	in situ polymerization—conventional painting technique	20.0—33.0	54
PU	2.44 mm	graphene	20 wt %	solution intercalation—solvent casting	17.0—20.0	55
PS		TrGO	2.24 wt %	solution mixing—solvent casting—compression molding	30.0	56
Epoxy	3.00 mm	3D grapheme Nanoplatelets (GNPs)/rGO		template method	30.0	57
PDMS	0.1 mm	graphene	10.00 wt %	solution mixing—solvent casting—microwave irradiation	130—134	58

Reproduced with permission from Orasugh et al.[3] Copyright 2022 Elsevier.

to the EM wave shielding. Conjointly because of the electrical continuity, continuous CF unit area is more practical in comparison to discontinuous CFs in EMI shields.[31]

The fiber-like platelike arrangement[33] and stacking arrangement[44] within the macroscale will greatly influence the SE. Figure 6 depicts the SE of three planar arrangements of a continuous carbon fiber chain consisting of ~12,000 fibers. With regard to arrangement 1, the chain is within a kind of a placoid coil, where the chain is continuous all over the coil. The chain in arrangement 2 is within parallel straight lines; such a chain is continuous between one line and the adjacent arrangement. In Figure 6, arrangements 2A and 2B match the chain direction, which is 0° and 90° apart on two reverse sides of the paper upon which the chain is attached. Hence, the 2A arrangement is delineated as unidirectional, and the 2B arrangement is defined as a cross-ply. Owing to its physical phenomenon and magnetism, Ni is an efficient coating material for CFs aimed at enhancing the SE.[23,32] Unglazed and nickel-glazed continuous CFs are compared with reference to the three planar prearrangements (Figure 6c).[33] As depicted in Figure 6a,b, the 2B arrangement offers an abundantly higher SE_T than 2A, whether or not the fiber is coated: this concurs with the way that

the EM waves are unpolarized. The unpolarized EM waves comprise the electrical field of EM waves directly centrifugally and haphazardly within the sample plane. It is very unremarkably applied relative to polarized EM radiation. Arrangement 1 offers a lower SE_T compared to its counterparts in arrangements 2A and 2B in uncoated fibers while providing a similar SE_T as arrangement 2A for the Ni-coated CFs. The inferiority of arrangement 1 to the second arrangement is clearer when the glaze is not applied. For sure, from magnetic attraction theory, the planar coil arrangement (as in arrangement 1) is more practical compared to the linear configuration (as in arrangement 2) with respect to magnetic interaction. Hence, the magnetic interface has less contribution to the shielding of EM waves over the electrical interface, although the magnetic interface is augmented once the fibers are coated with Ni.[25,32,33]

With regards to the unidirectional arrangement 2A, SE_T specifies that the electrical field interaction is greater in comparison to the magnetic field; meaning, arrangement 2A offers better SE compared to arrangement 1 with reference to the uncoated fibers. The cross-ply arrangement 2B offers much more interfacial interaction with the electrical field compared to arrangement 2A. Consequently, arrangement 2B offers abun-

dantly greater SE_T and SE_A than its counterpart (arrangement 2A) for unglazed and Ni-glazed fibers (Figure 6).[32,33]

Hybrid-based (nano)composites comprising two or more fillers are expected to exhibit superior EMI shielding properties compared to their counterparts having just one variety of reinforcing active or nonactive material, e.g., dual reinforcing filler may be fibers and/or particles.[34] Owing to the massive ratio of the fibers in comparison to particles, the existence of fibers augments the electrical connectivity within the (nano)-composite.

Multiscale (nano)composites (multifunctional composites) involving the amalgamation of diverse fillers of varying scales have currently been engaged by researchers globally. For example, fillers like microcarbon "mC" (CFs) and nC (CNTs) have been greatly utilized: the microcarbon is continuous whereas the nC is not continuous, and the inclusion of nC to mC might not end in a considerable improvement of the SE,[32,35] because of the dominating SE of the continual fibers. In the meantime, the mechanical characteristics are unrivaled for continuous C-nanocomposites compared to noncontinuous counterparts; the expansion of an irregular nC to continuous mC results in reduced wt % of the well-connected microcarbon therefore decreasing the composites' mechanical properties or even conjointly decreasing the shield's SE.[32] The effect of the reinforcing filler should be considered within the panache of a multifunctional hybrid/composite structure. As our focus is on graphene-based polymer composite materials, selected literature reports of such materials are shown in Table 3.

3.1.3. Ceramics. Ceramic materials, when compared with carbon or metals, are less commonly used materials to fabricate EMI shields primarily considering their low conductivity comparatively. Among ceramic materials, metal carbides are reasonably adopted for their conductive ability. Of the same kind as magnetic metals, ceramic magnetic materials are extremely effective as EM wave shields as a result of absorption. Examples are ferrite (Fe_3O_4, also called magnetite)[59,60] and nickel ferrite ($NiFe_2O_4$),[61] known to be ferrimagnets. Nonconductive ceramics having magnetic properties are preferred over metallic counterparts because of their corrosion-resistant properties. In this way, the amalgamative utilization of ceramics like Fe_3O_4 with the inclusion of conductive entities like metals or carbon (rGO, CNFs, or CNTs)[59] and/or inherently conducting polymers like PEDOT should prove effective.[60] Characteristically, the magnetic, polarizability, and nonconductive properties of ceramics alone make them ineffectual as EMI shields. Accordingly, research on earthenware production for EM wave shielding generally includes carbon−ceramic or clay−metal (nano)composites. Systems that incorporate bifillers like carbon−ceramic mixes[62] are silver−ceramic,[63] ceramic−FeS-iAl,[64] and Al_2O_3−metal.[64] Also, owing to this system's capability to stand high-temperatures, it is useful for high temperature shields, like SiC−C,[65] and Ti_3AlC_2[66] nanocomposites.[67] High permittivity of ceramics (perovskite) is eye-catching.[68,69] SiC−C,[69] SiC (nanowire), SiC−Si_3N_4,[70] and SiC−SiCN[66] are among the reported structural-based EMI shields per the literature. MXenes (2D inorganic materials), having good conductivity (4000 S/m), polarizability, and large surface area, are an emergent categorie of ceramic materials made of a small number of atoms thick 2-layer transition metal carbides, metal carbonitrides, metal nitrides, etc., which presents them as excellent materials for the fabrication of EMI shields.[71,72] Per the literature, MXene-based materials have presented SE of ≤24 dB,[71] 50−75 dB,[72] 70 dB,[73] 66−69 dB,[74] etc., within frequencies

of 8.2−12.4 GHz. The SE values of MXene shields (≥50 dB) are comparably lower than those of carbon-based materials. Literature reports inexpensive continuous-glass fibers as being nonconductive and having poor EMI shielding properties. Consequently, glass fiber-based polymeric matrix (nano)-composites are largely adopted for cheap structures like boats, concrete edifices, wind turbines, etc. Impacting glass fibers with EM wave shielding properties entails coating/adding conductive entities like CNT and CNFs to polymeric matrices.[75] An associated report communicated the glazing of glass fibers with conductive constituents like Ni and rGO,[76] which has also been adopted for microsphere-based hollow glass fibers.[77] Glass fibers also provide radiation transmitting coating to moderate the impedance mismatch.[78]

3.1.4. Cement-Based EMI Shielding Materials. Within the void of solid aggregates, cement is thought of as cement paste when a natural process is adopted. The mortar could be cement-based containing fine particle combinations, but no granular combination. This fine combination is often sand-based, while the coarse combination is often stone-based/gravel-based. The whole combination comprises reinforcing materials and additionally functions to help in reducing the material shrinkage effected by drying.[6]

Concrete admixtures are the constituents aside from water, cement along with aggregates, which are used during a cement amalgamation to boost definite properties in the interior of the cured cement material. The solid mixtures are noncontinuous materials as continuous fibers cannot be inclusively incorporated during a cement mixing process in their continuously aligned form. Cement shielding systems are ineffective as EMI shields except when the admixtures are capable of enhancing the shields' SE.

EMI shield-augmenting concoctions are principally conductive diminutive fibers (like CFs, CNTs, and/or steel-fibers) and semiconductive fillers (like coke, C, graphene, graphite, nickel, etc.). C falls within the kind of nanoparticle aggregate and it is much more cost-effective than CFs and CNTs. These systems reduced price is necessary toward fabricating concrete materials. EMI shielding components are presently led by C materials, particularly CFs,[79] CNTs,[80] C,[81] coke,[82] etc.

Ceramic nano/microparticles like Fe_2O_3 containing ash are an alternative sort of EMI shielding-augmenting compounds, though semiconductive blends' extent of providing enhanced EMI SE is better than ash by far.[81,83,84]

Adoption of the discontinuous fibers/particles for the fabrication of continual conducting routes aids the SE of these materials. The dispersive distribution of reinforcing fibers/particles in a cement admixture presents a great challenge, predominantly in an instance where the fiber/particle size is nanoscale. An instance is CNFs which get entangled, making their dispersion challenging in comparison to CFs.[85]

Nanoscale-based amalgamations as composites result in reduction of the air voids within the final product, a decrease necessary for enhancing the mechanical properties. Though the decrease in void % is vital for enhancement in mechanical properties, the utilization of an innovative nanofiller like CNTs for this purpose is not economical, because of the similar impact of carbon, which is way less costly than CNTs. The inclusion of nanofillers for advanced SE could also be partly responsible for the reduction of the air voids within the composite system. In consequence, the enhancement in the SE of nanofiller reinforced nanocomposite systems is chiefly based on the interfiller interfacial interaction with themselves and the EM waves.
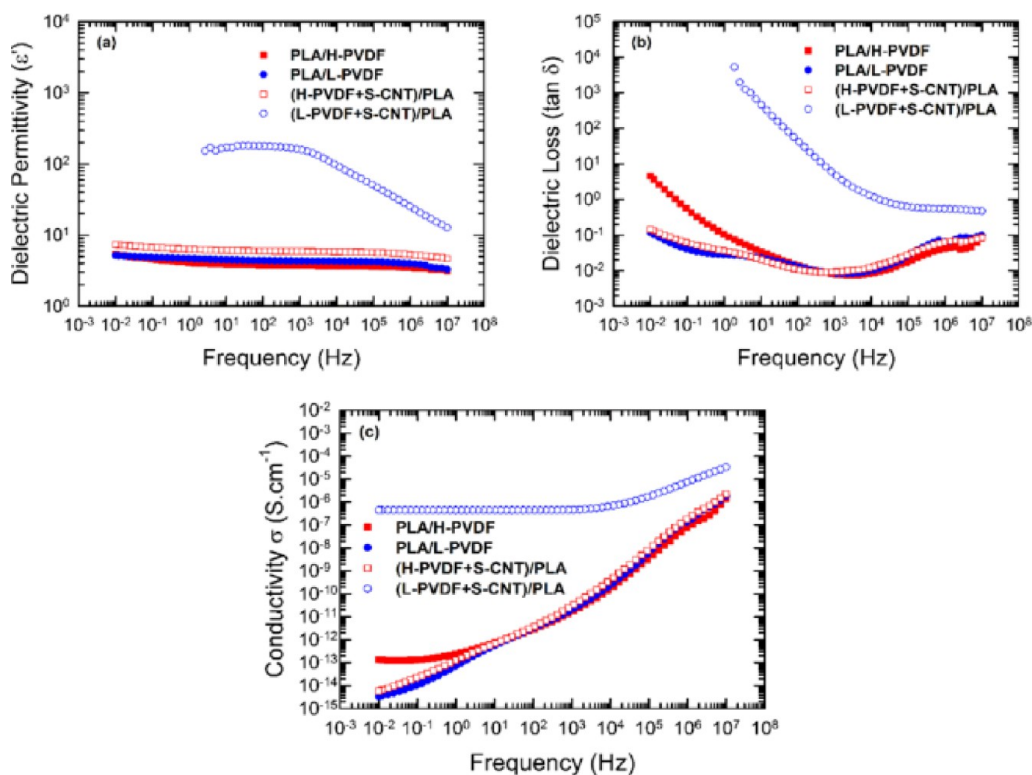
Figure 7. Dielectric (a) permittivity (ε'), (b) loss (tan δ), and (c) electrical conductivity (σ; S·cm^{-1}) of the (H-PVDF + S-CNT)/PLA and (L-PVDF + S-CNT)/PLA blend nanocomposites prepared from a two-step process. H-PVDF, high-density PVDF; L-PVDF, low-density PVDF; S-CNT, short CNTs (low aspect ratio). Reproduced with permission from ref 1. Copyright 2019 American Chemical Society.

The challenge associated with nanoparticle dispersion aforementioned can be mitigated by incorporating nSiO$_2$ (size 0.1 μm) added to the admixture cement. nSiO$_2$ could be obtained as a waste product; thus, it is cheap.

On the other hand, steel microfibers (diameter 8 mm and length 6 μm) having high surface area generally have an enormous diameter, making their interaction with EM waves high and consequently producing good SE of ~70 dB for 0.72 vol % in a cement-based system, whereas the SE for flat stainless steel 304 material having a thickness of 4.12 mm is ~78 dB.[84] In view of that, steel fiber cement is substandard to plate-like stainless steel having the same thickness as EMI shields. Steel microfiber's supremacy over CMFs (carbon microfibers) in augmenting SE of cement materials is associated with its high conductivity in comparison to the CMFs.[81] CFs possess a typical size and are coated with suitable organic compounds toward enhancing their processability in cement systems; unsized CMFs are mostly used in this fashion.[84] The SE clearly will increase with increasing fiber vol %. At constant CF vol %, the SE is comparable between mortar and cement paste.[84]

3.1.5. Polymers and Their Composites/Hybrids. Conventional polymeric materials are nonconductive and mainly transparent to EM radiation. Nevertheless, metal-encapsulated composite fibers are efficient as EM shields, with even better effectiveness in comparison to unencapsulated CFs.[31] On the other hand, inherently conductive polymers produced via modification of existing nonconductive polymers or direct synthesis from standard monomers possess conductive properties, making them valuable candidates for EMI shielding materials.[81] Examples include polypyrrole (PPy), polyacetylene (PA), polyindole (PIn), polyaniline (PANI), and their copolymers. Still, these polymers have a tendency to be disadvantaged by their characteristic mechanical properties inferior to those of standard polymeric matrices; additionally, they are costlier.[6] Polymers are the main matrices used as binding materials in nanocomposites/composites for EMI/EM wave shielding materials. Conductive polymer matrices are adopted in this vein considering their ability to enhance the thermal and electrical conductivity along with electrical continuity within the entire composite structure.[86] Conducting polymeric matrices are also utilized as supplementary components in nonconducting nanocomposites/composites in order to provide these systems with enhanced SE.[6,87] On the whole, the ability of a polymeric matrix or its rosin to permit effective dispersal of fillers aimed at enhanced EM wave shielding is vital toward effective employment of the reinforcing filler: filler dispersion conjointly affects the conduction of the nanocomposite. Polymer matrices having good resilience are essential for EMI seals.

The application of composite materials to fabricate EMI shielding materials has been broadly utilized by researchers globally (see Table 3).[10,88] One such example is studies performed on CNTs in PLA/PVDF composites along with their impact on the EMI SE, EC, and rheological performance.[1] These authors showed that the processing time, PVDF viscosity, aspect ratio of CNTs, and processing technique greatly affected the EMI SE of the final composite materials. They revealed in their study that SE of the composites/blends containing CNTs was better/higher than that of the blends without CNTs; they proved that the same trend was observed for the dielectric permittivity (ε'), dielectric loss (tan δ), and EC (σ; S·cm^{-1}) as in Figure 7.[1]

Zhang et al.[8] have also reported in their studies an innovative approach for converting a guest material into a host, producing
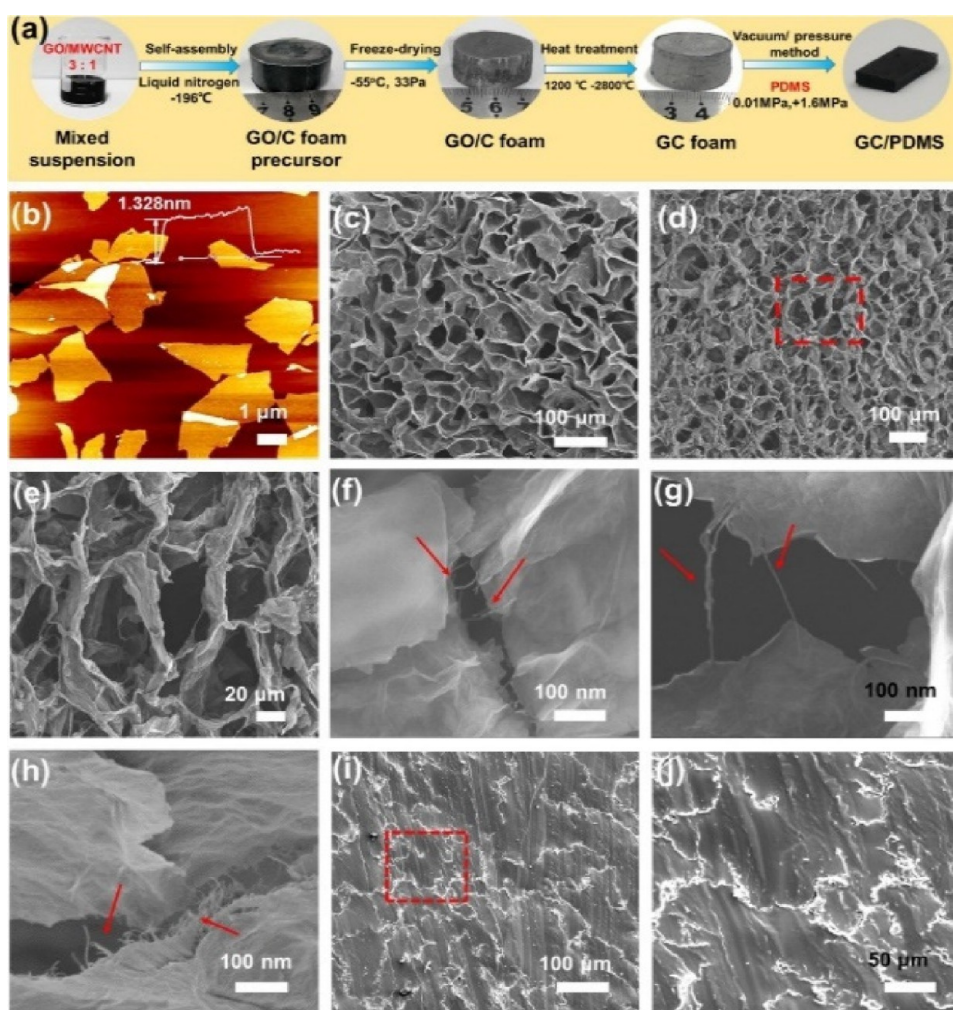
Figure 8. (a) Schematic illustration of preparation procedure of GC foam and GC/PDMS composite. (b) AFM image of initial GO sheets. (c) SEM image of initial GO/C foam. (d, e) SEM images of GC foam at different magnifications. (f, g) SEM images of MWCNTs' different distribution state in the 3D skeleton. (i, j) Cross-sectional SEM images of GC/PDMS composites at different magnification (bright parts are graphene sheets and MWCNTs, dark parts are PDMS matrix). Reproduced with permission from ref 23. Copyright 2020 Elsevier Science Ltd.

the unique WS_2 (tungsten disulfide)−rGO mountain-like structural wall possessing efficient and green EMI SE. They reported SE ≥ 20 dB within a frequency range of 2−18 GHz, and the maximum EMI SE they obtained was 32 dB along with an appealing green index, gs ≈ 1.0. The effective green EMI SE obtained in their work was credited to the multilevel architecture along with inherent dielectric properties of the fabricated WS_2−rGO structure, plus the relaxation and conduction synergy, along with multiscattering among the voids and interface, and the corresponding wedge effect.[8]

Jia et al.[23] in their work obtained SE_T as high as 54.43 dB and SS_E of 87.86 dB·cm^3/g within the X-band at ≤0.98 wt % filler loading for highly porous high-performance 3D graphene/CNT/polydimethylsiloxane nanocomposites (using a simple process as shown in Figure 8).

3.1.5.1. Structural Order for Polymer-Based Nanocomposites/Composites for EMI Shielding. With reference to Schelkunoff theory, EM wave shielding materials having isolated structural architecture and foam-based structure encourage multireflection along with attenuation of EM waves within the material structure, which is a boundless advantage to the enhancement in SE of structural materials.[89] Structural order for polymer-based nanocomposites/composites for EMI shielding

encompasses uniform structure,[90−92] segregated structure,[93,94] foamed structure,[95] and layered structure[44,96] as depicted in Figure 9.

Regarding the deliberations about enhancing the SE_R and SE_A of EMI shields, the architectural design of these materials affects their macrostructure, microstructure, nanostructure, and/or amalgamation and is a vital way to attain high SE. Hence, an effective conductive filler is not the only factor to be considered, but the structural design will also greatly influence the EMI shielding ability of the fabricated shield. Exceptional conductive attributes and good conductive networked structures are major prerequisites in the design, fabrication, and application of EM shielding nanocomposites/composites to obtain high SE, efficient multi-interfacial absorption and reflection, along with hysteresis loss features of the materials being imperative factors toward attaining high and controllable shielding performance of EMI shielding nanocomposites. Consequently, progressively more consideration has been given to the architectural design tuning of EMI composite shields.[1−5,91−96,98] Polymer materials' excellent plasticity and ease of processing play a progressively vital role in the EMI shielding composite's structural design.[1−5] These structures are categorized into uniform, segregated, foamed, and layered forms as aforementioned.
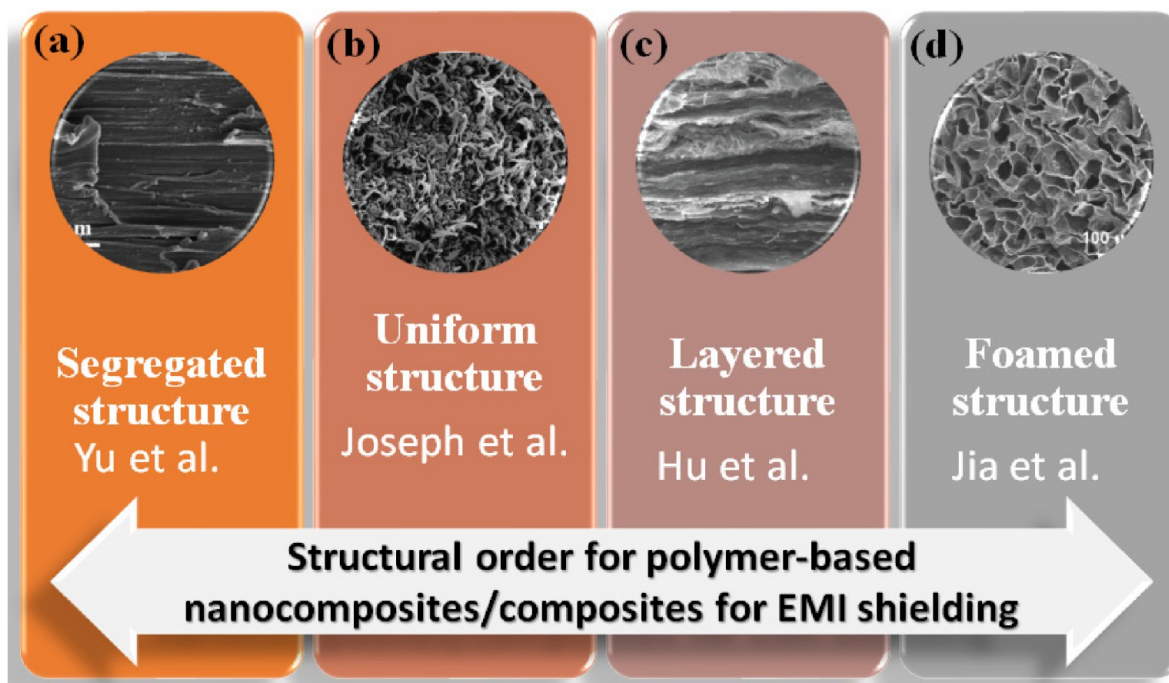
Figure 9. Scheme showing structural order for polymer-based nanocomposites/composites for EMI shielding materials: (a) segregated structure, (b) uniform structure, (c) layered structure, and (d) foamed structure. Reproduced with permission from refs 23, 92, 93, and 97, Jia et al., Joseph et al., Yu et al., and Hu et al. Copyright 2020, 2013, 2018, and 2022 Elsevier Science Ltd.

3.1.6. Other EM Wave Shields. Considering the continued advancement of human civilization within the field of nanotechnology, an ever-increasing number of new sorts of EMI shields are found and combined in progression, presenting new ways toward the improvement of EM wave shielding and fascinating materials. The systems possess unique structures along with lightweight features, which could deftly change or govern the EM wave shielding properties of these materials through suitable fabrication approaches and part configuration, making it possible to obtain a variety of different high-strength and lightweight innovative materials having tunable EM boundaries.

MXene, a comparatively innovative and novel 2D material, first announced in 2011, presents a metal-like conductive character like transition metal carbides chiefly attributed to −OH or terminal oxygen presence on its surface;[99] hence, its application in EMI shields has drawn wide consideration.

Various investigations demonstrate that MXene-based hybrids/nanocomposite systems like titanium carbide/ MXene,[100] AgNW/MXene nanowire,[101] MXene/aramid,[102] and MXene/CNF/silver[103] present exceptional EMI SE. In particular, diverse Ti_3C_2Tx MXene was fabricated by particle grafting; then, permeable 3D Ti_3C_2Tx MXene/C having assorted Ti_3C_2Tx MXene material thickness was synthesized by compounding with epoxy toward acquiring MCF/epoxy nanocomposite EMI shields. The subsequent MCF/epoxy nanocomposites displayed a superior EC of 184 S/m along with an extreme EMI SE of 46 dB, being 3.1×10^4 and 4-times greater than MCF/epoxy composites without Ti_3C_2Tx MXene. These authors observed that higher thickness of Ti_3C_2Tx MXene was directly proportional to the corresponding EMI SE.[104] Furthermore, the EM wave shielding performance of MCF/epoxy nanocomposites was chiefly attributed to SE_A, even though SE_R was also weak.[104] Special 3D conductive organizations of MCF could boost the extensive utilization of

MXene nanocomposite systems for the preparation of cutting-edge EMI shields. Specialists have researched the connection between MXene system (especially sheets) EC along with their EMI SE and presumed that MXene EC could be changed by changing their thickness/composition.[105] With regards to metal−matrix nanocomposites/composites and carbon materials utilized for EMI shielding as of late, the vast majority of them require a specific component layer thickness (≥0.1 mm) to accomplish viable EMI SE.

Interestingly, MXene EMI SE could adequately achieve up to 20 dB even at a thickness of ~40 nm. Nanocomposites made of MXene systems present endless potential outcomes to the lightweight characteristics of EMI shields. According to the viewpoint of "waste to abundance" and feasible turn of events, it is extraordinary to plan and fabricate EMI shields from waste biomass or homegrown waste. As the most well-known bundling material, layered board, has a low reuse rate in the wake of disposal, causing genuine contamination of the climate. Considering the uncommon construction of layered paperboard (crisscross collapsed structure sandwiched between two equal planes), a group of scientists designed and fabricated a carbonized corrugated board (CCB, 0.07−0.17 g/cm³ thick) composite system for lightweight EMI shields prepared via direct carbonization along with epoxy coating as support.[106] The prepared material presented an astounding EMI SE of ~46.0− 82.0 dB.[106] From another group of researchers,[106] hollow straw permeable CNT clusters (SCAs) have been manufactured by straight carbonization of wheat straw followed by efficient gathering. SCAs with a thickness of just around 33−72 mg/cm³ display magnificent EMI SE (~44−57.7 dB), which principally relies upon the dielectric loss and solid reflection loss (within porous cell structures). Further, GO aerogel (GA) is full of pores in the GA/SCA nanocomposite structure. The EMI SE of GA/ SCA nanocomposites was enhanced to ~66.1−70.6 dB contrasting with unadulterated SCAs.[107]
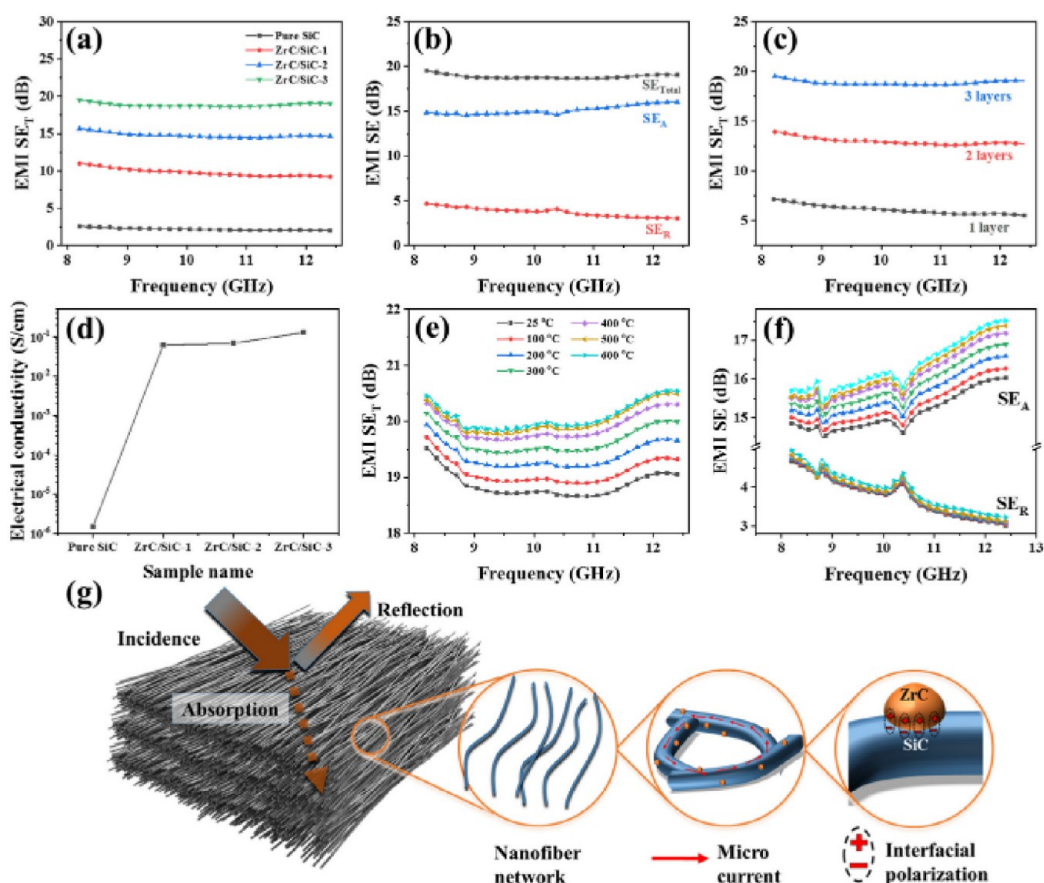
Figure 10. (a) EMI SE$_T$ of pure SiC fiber and ZrC/SiC nanofiber mats (3 layers, 1.8 mm) at room temperature; (b) comparison of SE$_T$, SE$_A$, and SE$_R$ for ZrC/SiC-3 sample (3 layers, 1.8 mm). (c) SE$_T$ of ZrC/SiC-3 samples with different thicknesses. (d) Electrical conductivity variations of pure SiC fiber and ZrC/SiC nanofiber mats. (e, f) EMI SE of pure SiC fiber and ZrC/SiC nanofiber mats (3 layers, 1.8 mm) at different evaluated temperature. (g) Schematic illustration of EM wave shielding for ZrC/SiC nanofiber mats. Reproduced with permission from ref 108. Copyright 2021 Elsevier Science Ltd.

We hope for something else, more innovative in this regard and more magnificent EMI shields to be found for a single polymer matrix or a blend of matrices toward innovative systems within the next decades.

4. EMI SHIELDING BEHAVIOR OF DIVERSE MATERIALS WITH RESPECT TO STRUCTURAL AND PERFORMANCE PROPERTIES ON THE SE AT COMBINATIONS OF FREQUENCY AND TEMPERATURE

Recently, a handful of researchers have shown interest in the study of the EMI shielding behavior of diverse shielding materials with respect to magnetic, filler, and conductivity behavior and the specific interfacial interactions on the SE at numerous combinations of frequency and temperature.[108,109]

A report from Hou et al.[108] reveals that environmental temperature can have a great influence on the average SE$_T$ at 25 °C to 600 °C and specific SE$_T$ at 25 °C being 18.9, 20.1, and 315.0 dB, at a material density of 0.061 g/cm^3. With the variation of the temperature from 25 to 600, these authors have revealed in their report a corresponding change in the SE$_T$ of the composite fiber mat (ZrC/SiC-3 nanofiber mat) they fabricated as shown in Figure 10.[108] This trend has been supported by other researchers.[109] Table 4 shows some of the reports from different research works. Mu et al.[109] have established in their work that an increase in temperature led to a corresponding
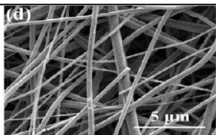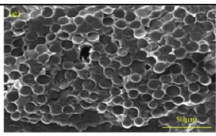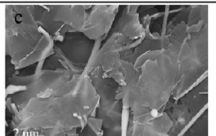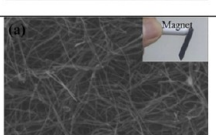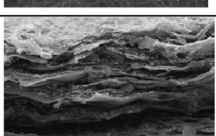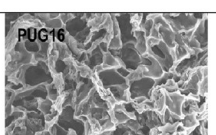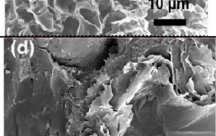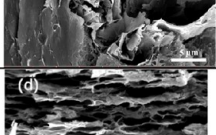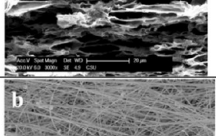
enhancement in the electrical conductivity and consequently the SE$_T$ of fabricated SiC$_f$/SiC composites as in Figure 11a,b, a trend supported by other scholars too as in Figure 10d.[39,108] The electrical conductivity of materials aimed at EMI shielding is a vital factor influencing the SE performance where the SE$_R$ and SE$_A$ are largely dependent on the electrical conductivity as expressed in the following equations (eqs 6 and 7):[6,107]

$$SE_R = 39.5 + 10 \log(\sigma/(2\pi f \mu)) \tag{6}$$

$$SE_A = 8.7 d \sqrt{\pi f \mu \sigma} \tag{7}$$

An innovative approach toward designing high-performance EMI shields by fabricating a stratified double-percolated architecture of PS/PVDF/MXene nanocomposites has been proposed by Wang et al.[114] where the S-PS/PVDF/M$_{12}$ nanocomposite (0.45 mm thick) exhibited EMI SE of 32.0 dB within the X-band while the H-PS/PVDF/M$_{12}$ nanocomposite (1.35 mm thick) exhibited 36 dB SE at a frequency of 10.51 GHz. They ascribed the chief influence on the SE to the enhanced absorption effectiveness being credited to the improved EC and robust multiple reflections along with less dipolar polarization loss.[114] A look at the afore-discussed works established that the thickness, number of layers, conductivity, structural morphology, density, and other undiscussed properties of materials aimed at EMI shielding application greatly influence the EMI SE ultimately. Researchers should carefully

Table 4. Structure and EMI Shielding Performance Reports of Different Materials As Per Literature[a]

Material	Density (g/cm³)	SE_T (dB) as per Temp. (°C)			Electrical conductivity (S/cm)	Surface/interface structure or morphology	Ref.
		Av. SE_T	Av. SE_T	Spec. SE_T dB cm³ g⁻¹			
		25 °C	600°C	25 °C			
ZrC/SiC-3 nanofiber mat	0.061	18.9	20.1	315.0	1.3×10^{-1}		108
Porous SiC foam	0.87	22.2	24.0	25.5	2070×10^{-4}		109
Graphene/ SiC_nanowire/PVDF composites	>1.78	29.4	-	<16.5	2.3×10^{-6}		110
SiC encapsulated Fe@CNT sponge	0.60	36.6	35.0	61.0	1.91		111
CNF/ TRGO@Ni film	-	25.1	-	32.2	262.7 S/m		112
multilayered PU graphene composites	-	17-21 single layer 23–24, multi-layered	-	-	~3.0 S/m		55
Graphene nanoplate (GNP)/carbonized loofah fibre (CLF)/polyether-ether-ketone (PEEK) composites	-	27.1	-	-	0.938 S/m		113
polystyrene (PS)/ polyvinylidene fluoride (PVDF)/ MXene composite	-	36	-	407	0.5		114
3D graphene microtubes membrane	0.0020-0.0036	28.55-38	-	10,556	-		115

Photographs reproduced with permission from Hou et al.,[108] Copyright 2021 Elsevier; Mu et al.,[109] Copyright 2015 Elsevier; Liang et al.,[110] Copyright 2020 Elsevier; Mei et al.,[111] Copyright 2019 Elsevier; Han et al.,[112] Copyright 2021 Elsevier; Li et al.,[55] Copyright 2017 Elsevier; Li et al.,[113] Copyright 2019 Elsevier; Wang et al.,[114] Copyright 2021 Elsevier; and Yin et al.,[115] Copyright 2020 Elsevier. "Frequency (GHz): 8.2−12.4.

consider the combination of these parameters when designing and fabricating an EMI shield.

A research report on CNF/TRGO@Ni (50 wt % reinforcement) which exhibited improved electrical conductivity up to
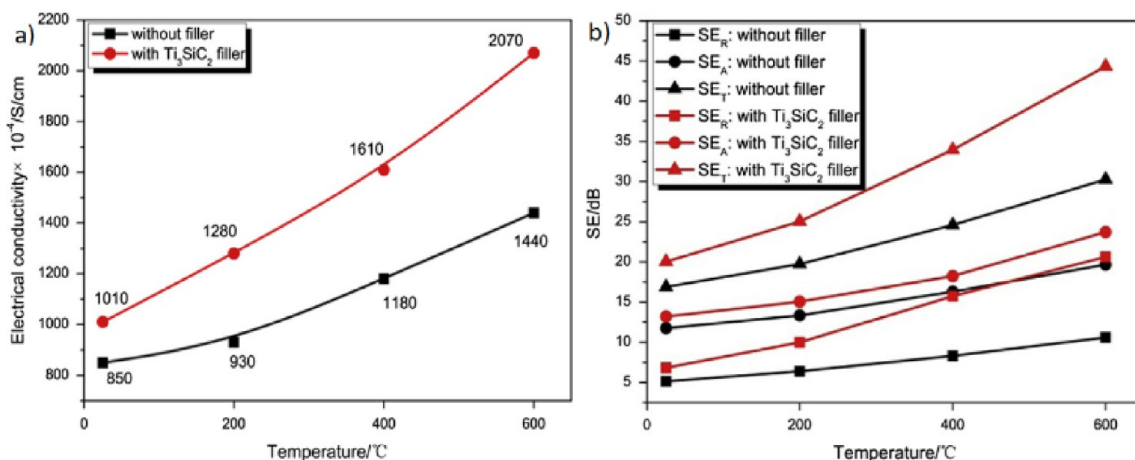
Figure 11. (a) DC electrical conductivity vs temperature of SiC_f/SiC composites without and with Ti_3SiC_2 filler and (b) variation of SE_A, SE_R, and SE_T at various temperatures of SiC_f/SiC composites with Ti_3SiC_2 filler. Reproduced with permission from ref 109. Copyright 2015 Elsevier Science Ltd.
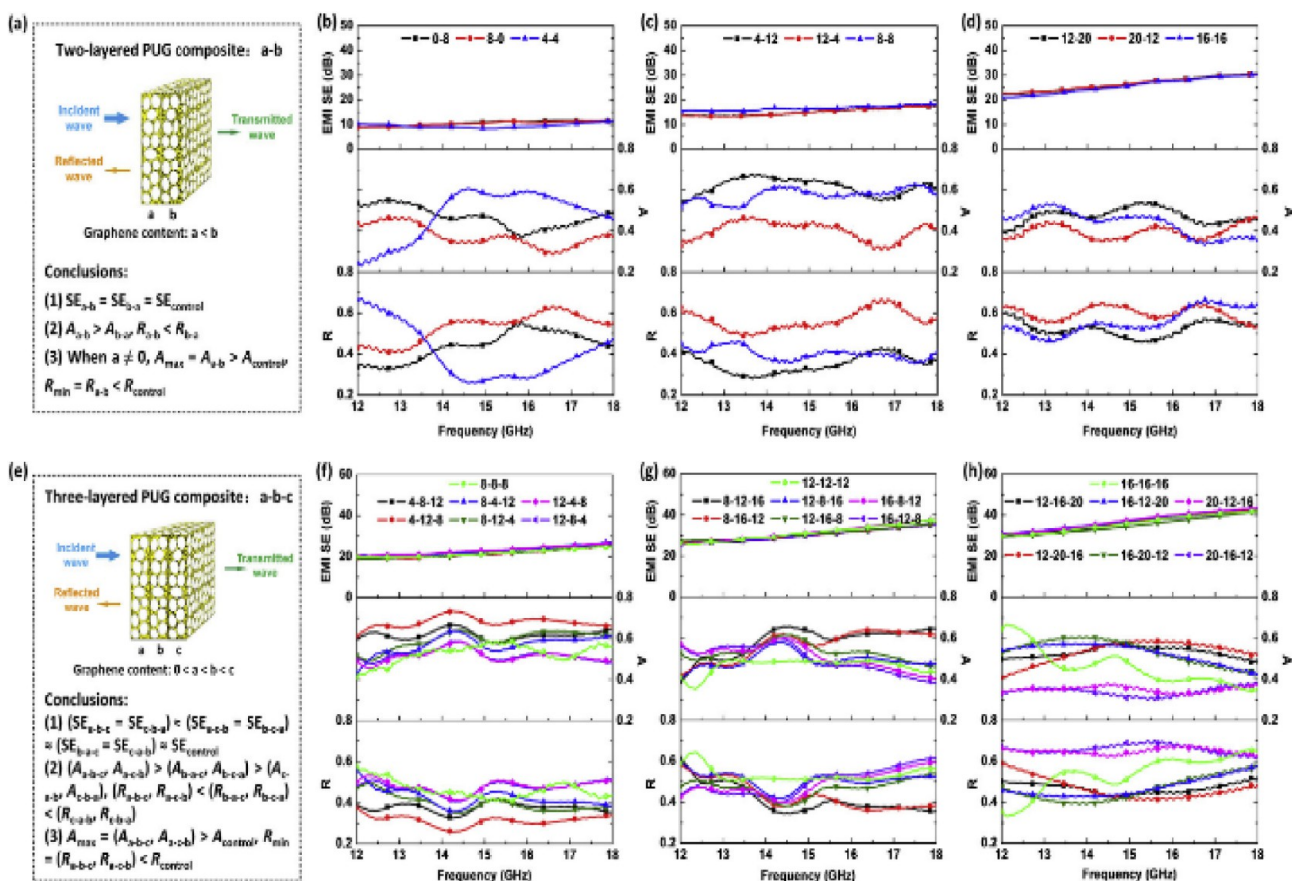

Figure 12. (a, e) Schemes of two- and three-layered PUG composites and conclusions resulting from panel b−d and f−h. (b−d) SE_T, SE_A, and SE_R of two-layered PUG composites in Ku-band: (b) 0−8, 8−0, and 4−4 (the control); (c) 4−12, 12−4, and 8−8 (the control); (d) 12−20, 20−12, and 16−16 (the control). (f−h) SE_T, SE_A, and SE_R of three-layered PUG composites in Ku band: (f) 4−8−12, 4−12−8, 8−4−12, 8−12−4, 12−4−8, 12−8−4, and 8−8−8 (the control); (g) 8−12−16, 8−16−12, 12−8−16, 12−16−8, 16−8−12, 16−12−8, and 12−12−12 (the control); (h) 12−16−20, 12−20−16, 16−12−20, 16−20−12, 20−12−16, 20−16−12, and 16−16−16 (the control). Reproduced with permission from ref 55. Copyright 2015 Elsevier Science Ltd.

262.7 S/m and EMI SE of 32.2 dB has been discussed.[112] The researchers also revealed that the composite exhibited excellent mechanical flexibility results such that the electrical conductivity and EMI SE only decayed by 7.5% after 1000 bending cycles. They attributed the EMI shielding mechanism to the combination of improved impedance mismatch, multireflection in "brick-mortar" lamellar structure, and bestowing of synergetic

loss by TRGO and Ni nanoparticles.[112] The number of layers of an EMI shielding material has been reported to highly influence the EMI SE at constant density and material composition.[55] Li and co-workers observed their materials' results as in Figures 12 and 13 and concluded that the gradient architecture had an incredible impact on the microwave-absorbing characteristics of polymeric matrix nanocomposites, in terms of their EMI SE, and
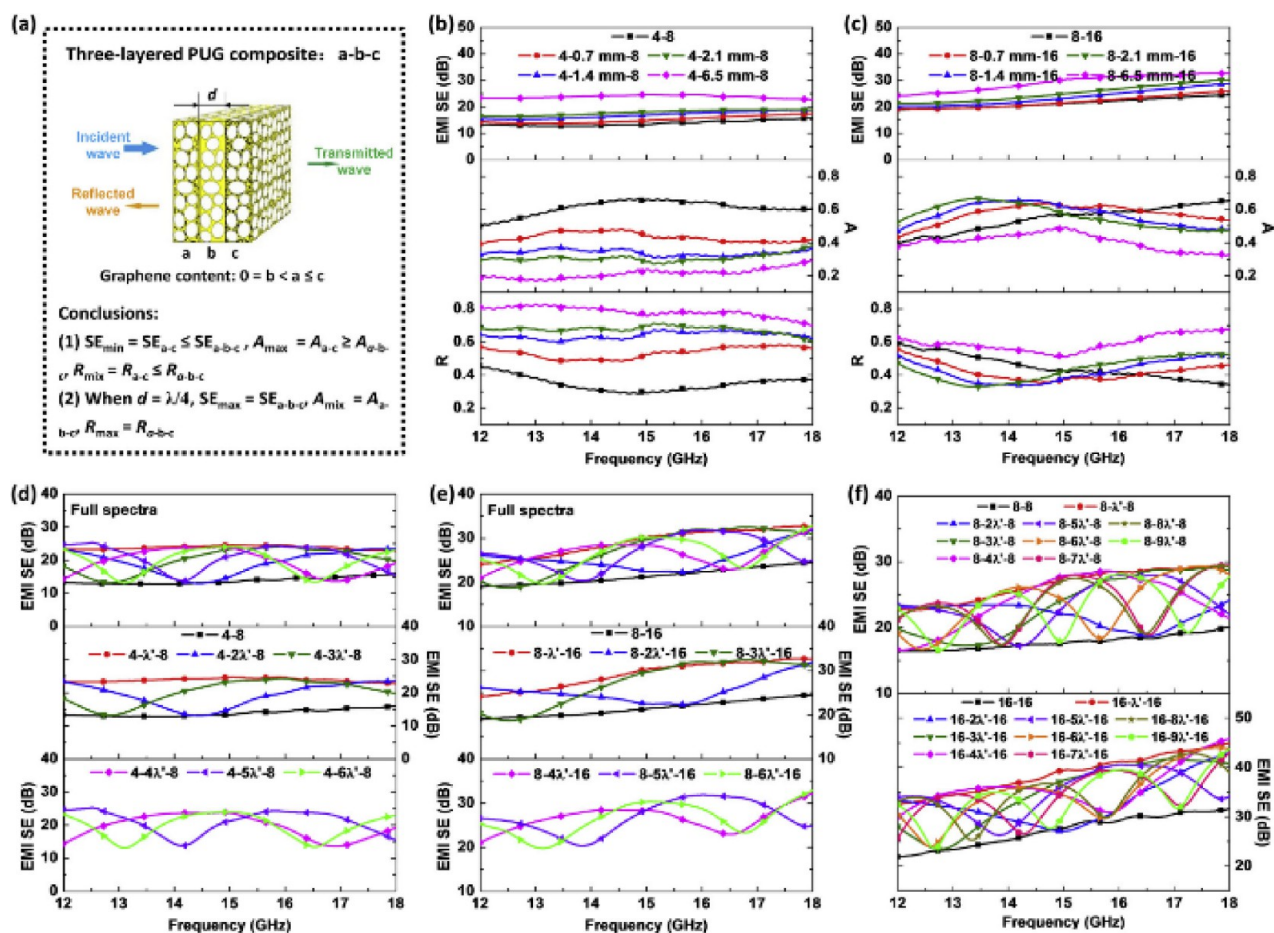
Figure 13. (a) Scheme of three-layered PUG composites with sandwich structure and conclusions resulting from panels b−f. (b, c) SE_T, SE_A, and SE_R of PUG composites with different thicknesses of interlayer in the Ku-band: (b) 4−8 (the control), 4−0.7 mm−8, 4−1.4 mm−8, 4−2.1 mm−8, 4−6.5 mm−8; (c) 8−16 (the control), 8−0.7 mm−16, 8−1.4 mm−16, 8−2.1 mm−16, 8−6.5 mm−16. (d−f) SE_T of PUG composites with the interlayer thickness of integral multiple of λ' in the Ku-band: (d) 4−8 (the control), 4−λ'−8, 4−2λ'−8, 4−3λ'−8, 4−4λ'−8, 4−5λ'−8, 4−6λ'−8; (e) 8−16 (the control), 8−λ'−16, 8−2λ'−16, 8−3λ'−16, 8−4λ'−16, 8−5λ'−16, 8−6λ'−16; (f) 8−8 (the control), 8−λ'−8, 8−2λ'−8, 8−3λ'−8, 8−4λ'−8, 8−5λ'−8, 8−6λ'−8, 8−7λ'−8, 8−8λ'−8, and 8−9λ'−8, and 16−16 (the control), 16−λ'−16, 16−2λ'−16, 16−3λ'−16, 16−4λ'−16, 16−5λ'−16, 16−6λ'−16, 16−7λ'−16, 16−8λ'−16, 16−9λ'−16. Reproduced with permission from ref 55. Copyright 2017 Elsevier Science Ltd.

there exists an optimum gradient architectural morphology capable of endowing the materials with the robust microwave-absorbing character; in comparison to gradient morphology/ structures, the sandwich architecture holds more advantages toward enhancing the SE of polymeric (nano)composites, and the augmented design helps the nanocomposites absorb extra EMI energy. Also, the enhancement in the SE of the nanocomposites with sandwich structure is attributed to the special morphological interference between two parallel-layered shields and is extremely reliant on the depth of the wave transmitting stratum d (Figure 13). When the d is 0 and $\lambda/4$, the equivalent SE values are at a minimum and maximum, correspondingly. The above-given information is decisive for the fabrication of high-performance polymeric nanocomposites with robust microwave-absorbing character.[55] Again, it is known that the gradient percentage of shield active components within the polymer nanocomposites is capable of increasing the dielectric constant more and more, thereby helping to diminish the reflected wave energy at the material boundary of the respective layers and increase the wave absorbed energy through conductive degeneracy.[55] Li et al. in their study of the EMI SE of GNP/carbonized loofah fiber CLF/PEEK nanocomposites established enhanced EMI SE of the nanocomposites implicitly

owing to the steady establishment of conductive-network morphology of CLF along with GNP;[113] where the shielding mechanism of the nanocomposites was attributed to absorption, as a result of the absorption contribution to the SE being much greater compared to the reflection.[113]

5. EMI SHIELDING MATERIAL APPLICATION AREAS

RWs (or MW radiation) are vital for telecommunication technology, together with global positioning systems (GPSs), antennas, radios, cell phones, Bluetooth technology (a wireless protocol for swapping knowledge/information between electronic/telecommunication devices), Wi-Fi (IEEE-802.11-based radiocommunication devices), and MW system devices.

EMI shielding systems are intimately associated with EM pulse (EMP) shielding systems. EMP refers to a transitory boosting of EM energy, like nuclear explosions or lightning strikes.

Exceedingly conductive substances typically for EMI shields are appropriate for antennas that conjointly perform within the radio wave and MW regimes. In the present civilized world, antennas are greatly required for wireless telecommunications appropriate for networking, autonomous automobiles, RF
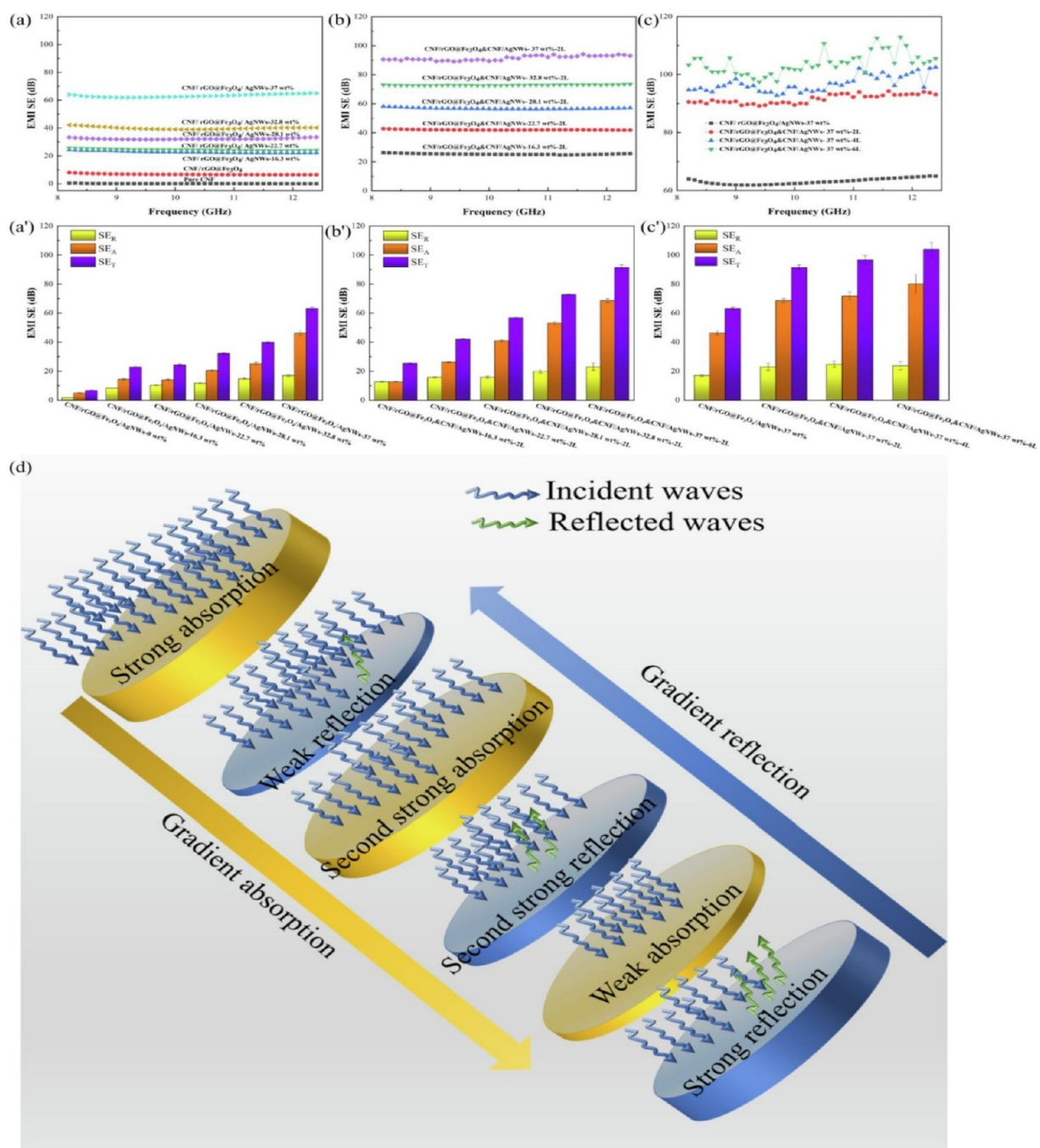
Figure 14. (a−c) EMI SE of blended nanocomposite films and asymmetric gradient alternating multilayer nanocomposite films at 8.2−12.4 GHz (X-band); (a′-c′) total EMI shielding effectiveness (SE_T), microwave reflection (SE_R), and microwave absorption (SE_A) of blended nanocomposite films and asymmetric gradient alternating multilayer nanocomposite films at 8.2−12.4 GHz (X-band); (d) Schematic diagram of electromagnetic wave propagation within CNF/rGO@Fe_3O_4&CNF/AgNWs-37 wt %-6L asymmetric gradient alternating 6-layer nanocomposite film. Reproduced with permission from ref 97. Copyright 2022 Elsevier Science Ltd.

identification device (RFID) labels, wearable (stretchable) smart devices, and virtual reality.

Conservative concrete systems have not at present developed to the level of replicating radio radiation shielding devices. Nevertheless, concrete-based materials have often demonstrated their potential via the inclusion of conductive elements (like CNF-reinforced compounds) to the concrete admixture.[87] This is helpful for the crosswise steering of automobiles on automatic highways.[87] As an example, the paving of the central part of a highway lane with RW-reflecting concrete material and inclusion

of a radio radiation transmitter and receiver on every automobile would allow detection of when the automobile is not traveling in the middle of its predetermined lane. By exploiting response management, the target automobile can be sustained within its lane, in that way realizing a programmed/automated steering system. The suggested approach is smarter than the substitute style of implanting magnets on the lane and controlling the automobile via sensing the force field.

6. DRAWBACKS IN THE ANALYSIS OF EMI SHIELDS

There exist various frequent downsides in the analysis of EMI shield targeted materials as addressed. One drawback is that the SE reports are lacking the SE_R or SE_A in many works. In a few instances, the SE_R report is not provided, while the SE_A is. A taxonomy problem relates to the usage of the term "reflection loss" with reference to the absorption loss where the reflection technique of SE_A measurement is adopted.[88]

Another drawback is that the SE per unit density and/or per unit thickness has been technologically considered more important than the SE. This is often not even reflective of technological desires. A high worth of SE per unit thickness permits a wafer-thin shield to produce sufficient SE. Yet, skinny materials are restricted to applications involving radiation predominantly at traditional incidence. Flexibility is efficacious for EMI shields for gaskets; however, terribly skinny shields do not exhibit resiliency adequate for shields requiring this character. The SE (better represented in terms of the absorption loss) per unit thickness portends to decline with growing shield thickness,[20] partly because of the result of the thickness on the microstructural architecture, as we know that the SE_A is directly associated with the shield's thickness. However, in reality, a straightforward correlation might not occur or may occur to some extent. The assumption of the quotient without acceptable experimental support could be a pitfall. Additionally, the fabric manufacturability might restrain the shield's thickness; hence a high worth of the SE cannot be attained despite a high worth of the SE per unit thickness. EMI shields (e.g., carbon-based shields) known to possess low density in comparison to metals are abundantly available. EMI shields that are exceptionally lightweight do not seem to be in vital technological demand.

Also, the absorption frequency dependence is a rumored but not an adequate rationalization of the comparatively advanced absorption loss frequency dependence.

An SE of 20 dB is adequate for a few applications, but considering the reported SE for varied materials (as high as 130 dB[25]), 20 dB is not a high level of shielding as the case of uncommonly high shielding is not even enough.

When the shielding testing technique is not represented, specifically also, the specimen/sample which is electrically associated with the waveguide and usually not represented, this is a significant drawback. Inadequate quality of this association may result in the escape of the incident EM waves by the side of the joint so that the estimated SE is not up to real-life worth.[25]

In the case of permeable EMI shields, the drawback is that the fraction of solid does not interact properly. This volume fraction is altered with modification of the material. For instance, the solid volume fraction will be changed with the inclusion of an extra entity (like graphene). Increased volume fraction unaided will also result in enhanced SE. A connected drawback is the SE within a unit solid volume fraction is not the same throughout.

Again, the discussion about the skin-effect by researchers is rare or not even performed. However, it is a fundamental material property providing insight into the SE, significantly for materials that do not seem to be magnetic.

Also, the variation in property within (anisotropy) the shielding material is not considered: this is because the material properties will occur among a plane and may conjointly take place in the plane and across the thickness. For instance, graphene flakes are more favorably aligned within the shield plane, therefore inflicting anisotropy sandwiched between in-plane and across the thickness routes. Also CFs are aligned in a specific plane within the shield direction; thus, anisotropy exists within the plane. The anisotropy affects the SE in the varied planes of the prevalence of the energy. The polarization of the incident radiation conjointly plays a part in the result due to anisotropy.

There is insufficient consideration of the macroscale structural architecture (e.g., the alignment of the CFs).[32] Primarily all attention has been given to microstructural or nanostructural architecture.

Another issue is that comparing with previous works is restricted to a definite frequency range, yet the art and performance are comparable over a broad range of frequencies. To advance the field, comparison with previous work ought to cover a broader frequency range.

A shortcoming in this regard is that the standards for material style aimed at attaining high SE do not seem to be adequately comprehended.

7. SUGGESTED WAY FORWARD

The combination of structural and functional properties during the design and engineering of an EMI shield should be the main drive for researchers working in the field of EMI shielding materials.

Structural and functional materials as EMI shields have attracted very negligible attention despite the high SE of continuous CF nanocomposites. Most attention has been channelled to their functional counterparts. For instance, in a recent report, Hu and his colleagues postulated and proved that the design and fabrication of a well-engineered gradient structure as depicted in Figure 14 would greatly enhance the SE of the shield.[97] They proved this concept by comparing the EMI SE of their film samples (Figure 14a) where they revealed EMI SE of 6.8 dB for the nanocomposite blend (CNF/rGO@Fe$_3$O$_4$). The SE obtained herewith was reportedly primarily caused by the efficient attenuation of electromagnetic waves by rGO@Fe$_3$O$_4$ via dielectric and magnetic losses. Also, the CNF/rGO@Fe$_3$O$_4$/AgNWs-37 wt % blended nanocomposite film had an average EMI SE of 63.1 dB compared to the CNF/AgNWs-37 wt % blended composite film's mean EMI SE of 31.2 dB, showing that the rGO@Fe$_3$O$_4$ and AgNW synergism improved EMI shielding effectiveness. The asymmetric 2-layer composite film showed higher EMI SE values than the blended composite with about the same composition as well as content, as shown in Figure 14b. Without altering the composition and other content of the CNF/rGO@Fe3O4&CNF/AgNW-37%-2L asymmetric 2-layer composite film, they prepared nanocomposite films with asymmetric gradient varying 4- and 6-layer structures to further enhance the EMI shielding performance of the asymmetric layered composite. As anticipated, the asymmetric gradient switching 4- and 6-layer structured composite films' EMI shielding characteristics were much better than those of the CNF/rGO@Fe3O4&CNF/AgNW-37 wt % asymmetric 2-layer composite film (Figure 14c) (average EMI SE of 91.6 dB).[97]

Figure 14d shows the schematic diagram of the electromagnetic wave transmission process used by the CNF/rGO@Fe$_3$O$_4$&CNF/AgNWs-37 wt percent −6L asymmetric gradient alternating 6-layer nanocomposite film, according to these scientists, in order to more effectively explain the unique EMI shielding mechanism. Due to the dielectric and magnetic losses of the rGO@Fe$_3$O$_4$, a portion of the electromagnetic waves that strike the strong absorption layer are absorbed, with a smaller portion being reflected.[97] A small percentage of the electro-

magnetic waves are reflected at the interface between the strong absorption layer and the weak reflection layer as a result of an impedance mismatch, and then the strong absorption layer reabsorbs the remaining electromagnetic waves as they pass through the weak reflection layer. Meanwhile, some of the electromagnetic waves that enter the weak reflection layer interact with high-density carriers (such as electrons, holes, and dipoles), which causes ohmic loss, attenuation of the energy of the electromagnetic waves by the induced current, and ultimately absorption of the electromagnetic waves. The correlation between experimental data and EM theory is insufficient. Primarily most present reports fail to provide this relationship.

Fewer electromagnetic waves are absorbed by the secondary strong absorption layer when electromagnetic waves passing through the weak reflection layer reach it because of magnetic loss as well as dielectric loss. A portion of the electromagnetic waves are reflected back to the secondary strong absorption layer, the weak reflection layer, and the strong absorption layer where they are absorbed as they pass through the secondary strong absorption layer as well as the secondary strong reflection sheet. Ohmic loss as well as the attenuation of the electromagnetic wave energy by the generated current cause a portion of the electromagnetic waves entering the secondary strong reflective layer to be absorbed by the layer.

Only a very small fraction of the electromagnetic waves are absorbed by the weak absorption layer as they pass through the second strong reflection layer due to magnetic loss and dielectric loss.

A portion of the electromagnetic waves is reflected back to the weak absorption layer, the second strong reflection layer, the second strong absorption layer, the weak reflection layer, and the strong absorption layer, where it is reflected and absorbed numerous times.[97] This happens when the electromagnetic waves passing through the weak absorption layer meet the strong reflection layer. Due to the significant ohmic loss and attenuation of the electromagnetic wave energy by the induction current, the residual electromagnetic waves inside the strong reflection layer are absorbed by the layer. The asymmetric gradient alternating 6-layer structure nanocomposite film's EMI SE is significantly increased by this special EMI shielding method, which subjects electromagnetic waves to continuous gradient reflection but also gradient absorption. As a result, the 6-layer nanocomposite structure with an alternating gradient pattern offers a useful method for creating electromagnetic shielding materials with exceptionally high electromagnetic shielding performance.[97]

We, therefore, postulate that, the effective design and engineering of novel gradient-based polymeric shielding materials without neglecting the structural as well as functional characteristics of the engineered shield will launch researchers within the field of EMI shields into a new era of functional materials which may also serve other needs such as UV shielding, energy materials, etc.

8. CONCLUSIONS

This article could be an all-inclusive but nonexhaustive review of important materials within the sphere of EMI shielding, to enhance the growth of this niche. Functional, structural, and multistructural shielding materials are herewith covered. Small-scale utilization of functional shielding materials gained the attention of researchers and industrialists recently, though structural shielding materials enable multifunctional structures in extensive applications. The shielding materials dominant among structural shielding materials are continuous carbon fiber hybrids/composites and their cement-based counterparts. These shielding materials include polymers, cement, ceramics, carbons, metals, hybrids, nanocomposites, etc. The dominant method adopted by researchers to fabricate these structures toward the enhancement of SE is through hybrids/nano-composites. Carbons and metals are the most functional materials for offering efficient SE, while polymers (non-conductive), ceramics, and cement are generally not effective unless combined with functional components/materials. None-theless, some ceramics (like Ti_3AlC_2, SiC, and MXene,) and intrinsically conducting polymers like poly(*para*-phenylene), polythiophene, PA, PANI, PPy, poly(phenylene vinylene), and polyfuran are conductive and efficiently effective as shielding materials to a large extent. Owing to the supply of various forms of microcarbons and nanocarbons, shielding materials such as cement−carbon, ceramic−carbon, metal−carbon, and/or poly-mer−carbon mixtures have received much attention recently. The philosophies of EMI shields, their design, and their fabrication are herewith discussed, with the consideration of the reflection and absorption loss contributions to shielding and the structural architecture (nanoscale, microscale, and macro-scale). Also, the drawbacks of EMI shielding materials research are discussed. These EMI shields are beneficial microwave and radio wave systems, too besides EMI SE.

■ AUTHOR INFORMATION

Corresponding Authors

Jonathan Tersur Orasugh − *Department of Chemical Sciences, University of Johannesburg, 2028 Johannesburg, South Africa; Centre for Nanostructures and Advanced Materials, DSI-CSIR Nanotechnology Innovation Centre, Council for Scientific and Industrial Research, Pretoria 0001, South Africa;* Email: JOrasugh@csir.co.za

Suprakas Sinha Ray − *Department of Chemical Sciences, University of Johannesburg, 2028 Johannesburg, South Africa; Centre for Nanostructures and Advanced Materials, DSI-CSIR Nanotechnology Innovation Centre, Council for Scientific and Industrial Research, Pretoria 0001, South Africa;* ⓘ orcid.org/0000-0002-0007-2595; Email: RSuprakas@csir.co.za, ssinharay@uj.ac.za

Complete contact information is available at:
https://pubs.acs.org/10.1021/acsomega.2c05815

■ REFERENCES

(1) Salehiyan, R.; Nofar, M.; Ray, S. S.; Ojijo, V. Kinetically controlled localization of carbon nanotubes in polylactide/poly (vinylidene fluoride) blend nanocomposites and their influence on electromagnetic interference shielding, electrical conductivity, and rheological properties. *J. Phys. Chem. C* **2019**, *123* (31), 19195−19207.

(2) Saini, P.; Aror, M. Microwave absorption and EMI shielding behavior of nanocomposites based on intrinsically conducting polymers, graphene and carbon nanotubes. *New polymers for special applications* **2012**, *3*, 73−112. Jose, G.; Padeep, P. Electromagnetic shielding effectiveness and mechanical characteristics of polypropylene based CFRP. *International Journal on Theoretical and Applied Research in Mechanical Engineering (IJTARME)* **2014**, *3* (3), 47−53. Schelkunoff, S. Ultrashort electromagnetic waves IV—guided propagation. *Electrical Engineering* **1943**, *62* (6), 235−246.

(3) Orasugh, J. T.; Pal, C.; Ali, M. S.; Chattopadhyay, D.Electromagnetic interference shielding property of polymer-graphene composites. *Polymer Nanocomposites Containing Graphene*; Elsevier, 2022; pp 211−243.

(4) Schulz, R. B.; Plantz, V.; Brush, D. Shielding theory and practice. *IEEE Transactions on Electromagnetic Compatibility* **1988**, *30* (3), 187−201.

(5) Joshi, A.; Datar, S. Carbon nanostructure composite for electromagnetic interference shielding. *Pramana* **2015**, *84* (6), 1099−1116.

(6) Chung, D. Materials for electromagnetic interference shielding. *Mater. Chem. Phys.* **2020**, *255*, 123587.

(7) Gebrekrstos, A.; Orasugh, J. T.; Muzata, T. S.; Ray, S. S. Cellulose-Based Sustainable Composites: A Review of Systems for Applications in EMI Shielding and Sensors. *Macromol. Mater. Eng.* **2022**, *307*, 2200185.

(8) Zhang, D.-Q.; Liu, T.-T.; Shu, J.-C.; Liang, S.; Wang, X.-X.; Cheng, J.-Y.; Wang, H.; Cao, M.-S. Self-assembly construction of WS2-rGO architecture with green EMI shielding. *ACS Appl. Mater. Interfaces* **2019**, *11* (30), 26807−26816.

(9) Sushmita, K.; Madras, G.; Bose, S. Polymer Nanocomposites Containing Semiconductors as Advanced Materials for EMI Shielding. *ACS Omega* **2020**, *5* (10), 4705−4718.

(10) Matula, R. A. Electrical resistivity of copper, gold, palladium, and silver. *J. Phys. Chem. Ref. Data* **1979**, *8* (4), 1147−1298.

(11) Gupta, S.; Tai, N.-H. Carbon materials and their composites for electromagnetic interference shielding effectiveness in X-band. *Carbon* **2019**, *152*, 159−187. Mederos-Henry, F.; Hermans, S.; Huynen, I. Microwave characterization of metal-decorated carbon nanopowders using a single transmission line. *J. Nanomater.* **2019**, *2019*, 3280461. Wang, L.; Tamainot-Telto, Z.; Metcalf, S.; Critoph, R.; Wang, R. Anisotropic thermal conductivity and permeability of compacted expanded natural graphite. *Appl. Therm. Eng.* **2010**, *30* (13), 1805−1811. Calebrese, C.; Eisman, G. A.; Lewis, D. J.; Schadler, L. S. Swelling and related mechanical and physical properties of carbon nanofiber filled mesophase pitch for use as a bipolar plate material. *Carbon* **2010**, *48* (13), 3939−3946.

(12) Du, Y.; Liu, T.; Yu, B.; Gao, H.; Xu, P.; Wang, J.; Wang, X.; Han, X. The electromagnetic properties and microwave absorption of mesoporous carbon. *Mater. Chem. Phys.* **2012**, *135* (2−3), 884−891.

(13) CEP Technologies Corporation*How Do Skin Effect and Skin Depth Impact EMI/RFI Shielding?*CEP Technologies Corporation, 2020. https://ceptech.net/how-does-skin-effect-and-skin-depth-impact-emi-rfi-shielding/ (accessed 12.04.2022).

(14) Shui, X.; Chung, D. Nickel filament polymer-matrix composites with low surface impedance and high electromagnetic interference shielding effectiveness. *J. Electron. Mater.* **1997**, *26* (8), 928−934.

(15) Shui, X.; Chung, D. Magnetic properties of nickel filament polymer-matrix composites. *J. Electron. Mater.* **1996**, *25* (6), 930−934.

(16) Liang, J.; Wang, Y.; Huang, Y.; Ma, Y.; Liu, Z.; Cai, J.; Zhang, C.; Gao, H.; Chen, Y. Electromagnetic interference shielding of graphene/epoxy composites. *Carbon* **2009**, *47* (3), 922−925.

(17) Ling, J.; Zhai, W.; Feng, W.; Shen, B.; Zhang, J.; Zheng, W. G. Facile preparation of lightweight microcellular polyetherimide/graphene composite foams for electromagnetic interference shielding. *ACS Appl. Mater. Interfaces* **2013**, *5* (7), 2677−2684.

(18) Menon, A. V.; Madras, G.; Bose, S. Magnetic alloy-MWNT Heterostructure as efficient electromagnetic wave suppressors in soft nanocomposites. *ChemistrySelect* **2017**, *2* (26), 7831−7844.

(19) Wu, J.; Chung, D. Combined use of magnetic and electrically conductive fillers in a polymer matrix for electromagnetic interference shielding. *J. Electron. Mater.* **2008**, *37* (8), 1088−1094.

(20) Guan, H.; Chung, D. Radio-wave electrical conductivity and absorption-dominant interaction with radio wave of exfoliated-graphite-based flexible graphite, with relevance to electromagnetic shielding and antennas. *Carbon* **2020**, *157*, 549−562.

(21) Heinß, J.-P.; Fietzke, F. High-rate deposition of thick aluminum coatings on plastic parts for electromagnetic shielding. *Surf. Coat. Technol.* **2020**, *385*, 125134.

(22) Xu, Y.; Uddin, A.; Estevez, D.; Luo, Y.; Peng, H.; Qin, F. Lightweight microwire/graphene/silicone rubber composites for efficient electromagnetic interference shielding and low microwave reflectivity. *Compos. Sci. Technol.* **2020**, *189*, 108022.

(23) Jia, H.; Kong, Q.-Q.; Liu, Z.; Wei, X.-X.; Li, X.-M.; Chen, J.-P.; Li, F.; Yang, X.; Sun, G.-H.; Chen, C.-M. 3D graphene/carbon nanotubes/polydimethylsiloxane composites as high-performance electromagnetic shielding material in X-band. *Composites Part A: Applied Science and Manufacturing* **2020**, *129*, 105712.

(24) Drakakis, E.; Suchea, M.; Tudose, V.; Kenanakis, G.; Stratakis, D.; Dangakis, K.; Miaoudakis, A.; Vernardou, D.; Koudoumas, E. Zinc oxide-graphene based composite layers for electromagnetic interference shielding in the GHz frequency range. *Thin Solid Films* **2018**, *651*, 152−157. Hong, S. Y.; Kim, Y. C.; Wang, M.; Nam, J.-D.; Suhr, J. Anisotropic electromagnetic interference shielding properties of polymer-based composites with magnetically-responsive aligned Fe3O4 decorated reduced graphene oxide. *Eur. Polym. J.* **2020**, *127*, 109595. Wahaab, F. A.; Yahya, W.; Adebayo, L. L.; Kazeem, I.; Abdulraheem, A.; Alqasem, B.; Yusuf, J. Y.; Adekoya, A. A.; Nyuk, C. M. Graphene@ Ni0. 5Co0. 5Fe2O4 hybrid framework with enhanced interfacial polarization for electromagnetic wave absorption. *J. Alloys Compd.* **2021**, *854*, 157259. Mirzaee, O.; Huynen, I.; Zareinejad, M. Electromagnetic wave absorption characteristics of single and double layer absorbers based on trimetallic FeCoNi@ C metal- organic framework incorporated with MWCNTs. *Synth. Met.* **2021**, *271*, 116634. Zhang, Y.-P.; Zhou, C.-G.; Sun, W.-J.; Wang, T.; Jia, L.-C.; Yan, D.-X.; Li, Z.-M. Injection molding of segregated carbon nanotube/polypropylene composite with enhanced electromagnetic interference shielding and mechanical performance. *Compos. Sci. Technol.* **2020**, *197*, 108253. Zhao, Y.; Hou, J.; Bai, Z.; Yang, Y.; Guo, X.; Cheng, H.; Zhao, Z.; Zhang, X.; Chen, J.; Shen, C. Facile preparation of lightweight PE/PVDF/Fe3O4/CNTs nanocomposite foams with high conductivity for efficient electromagnetic interference shielding. *Composites Part A: Applied Science and Manufacturing* **2020**, *139*, 106095. Han, L.; Song, Q.; Li, K.; Yin, X.; Sun, J.; Li, H.; Zhang, F.; Ren, X.; Wang, X. Hierarchical, seamless, edge-rich nanocarbon hybrid foams for highly efficient electromagnetic-interference shielding. *Journal of Materials Science & Technology* **2021**, *72*, 154−161. Han, C.; Zhang, M.; Cao, W.-Q.; Cao, M.-S. Electrospinning and in-situ hierarchical thermal treatment to tailor C-NiCo2O4 nanofibers for tunable microwave absorption. *Carbon* **2021**, *171*, 953−962. Tao, J.; Zhou, J.; Yao, Z.; Jiao, Z.; Wei, B.; Tan, R.; Li, Z. Multi-shell hollow porous carbon nanoparticles with excellent microwave absorption properties. *Carbon* **2021**, *172*, 542−555. Patle, V. K.; Kumar, R.; Sharma, A.; Dwivedi, N.; Muchhala, D.; Chaudhary, A.; Mehta, Y.; Mondal, D.; Srivastava, A. Three dimension phenolic resin derived carbon-CNTs hybrid foam for fire retardant and effective electromagnetic interference shielding. *Composites Part C: Open Access* **2020**, *2*, 100020. Hou, S.; He, S.; Zhu, T.; Li, J.; Ma, L.; Du, H.; Shen, W.; Kang, F.; Huang, Z.-H. Environment-friendly preparation of exfoliated graphite and functional graphite sheets. *Journal of Materiomics* **2021**, *7* (1), 136−145.

(25) Luo, X.; Chung, D. Electromagnetic interference shielding reaching 130 dB using flexible graphite. *MRS Online Proceedings Library* **1996**, *445* (1), 235−238.

(26) Wang, P.; Guo, B.; Zhang, Z.; Gao, W.; Zhou, W.; Ma, H.; Wu, W.; Han, J.; Zhang, R. Eco-friendly non-acid intercalation and exfoliation of graphite to graphene nanosheets in the binary-peroxidant system for EMI shielding. *Chin. Chem. Lett.* **2021**, *32* (11), 3469−3473.

(27) Zhang, D.; Yang, H.; Pan, J.; Lewis, B.; Zhou, W.; Cai, K.; Benatar, A.; Lee, L. J.; Castro, J. M. Multi-functional CNT nanopaper polyurethane nanocomposite fabricated by ultrasonic infiltration and dip soaking processes. *Composites Part B: Engineering* **2020**, *182*, 107646.

(28) Lan, C.; Guo, M.; Li, C.; Qiu, Y.; Ma, Y.; Sun, J. Axial alignment of carbon nanotubes on fibers to enable highly conductive fabrics for electromagnetic interference shielding. *ACS Appl. Mater. Interfaces* **2020**, *12* (6), 7477−7485.

(29) Wan, C.; Jiao, Y.; Li, X.; Tian, W.; Li, J.; Wu, Y. A multi-dimensional and level-by-level assembly strategy for constructing flexible and sandwich-type nanoheterostructures for high-performance electromagnetic interference shielding. *Nanoscale* **2020**, *12* (5), 3308−3316.

(30) Kim, T.; Chung, D. Mats and fabrics for electromagnetic interference shielding. *J. Mater. Eng. Perform.* **2006**, *15* (3), 295−298.

(31) Luo, X.; Chung, D. Electromagnetic interference shielding using continuous carbon-fiber carbon-matrix and polymer-matrix composites. *Composites Part B: Engineering* **1999**, *30* (3), 227−231.

(32) Guan, H.; Chung, D. Effect of the planar coil and linear arrangements of continuous carbon fiber tow on the electromagnetic interference shielding effectiveness, with comparison of carbon fibers with and without nickel coating. *Carbon* **2019**, *152*, 898−908.

(33) Chung, D.; Eddib, A. A. Effect of fiber lay-up configuration on the electromagnetic interference shielding effectiveness of continuous carbon fiber polymer-matrix composite. *Carbon* **2019**, *141*, 685−691.

(34) Micheli, D.; Vricella, A.; Pastore, R.; Delfini, A.; Giusti, A.; Albano, M.; Marchetti, M.; Moglie, F.; Primiani, V. M. Ballistic and electromagnetic shielding behaviour of multifunctional Kevlar fiber reinforced epoxy composites modified by carbon nanotubes. *Carbon* **2016**, *104*, 141−156.

(35) Yao, K.; Gong, J.; Tian, N.; Lin, Y.; Wen, X.; Jiang, Z.; Na, H.; Tang, T. Flammability properties and electromagnetic interference shielding of PVC/graphene composites containing Fe 3 O 4 nanoparticles. *Rsc Advances* **2015**, *5* (40), 31910−31919.

(36) Eswaraiah, V.; Sankaranarayanan, V.; Ramaprabhu, S. Functionalized graphene-PVDF foam composites for EMI shielding. *Macromol. Mater. Eng.* **2011**, *296* (10), 894−898.

(37) Shen, B.; Li, Y.; Zhai, W.; Zheng, W. Compressible graphene-coated polymer foams with ultralow density for adjustable electromagnetic interference (EMI) shielding. *ACS Appl. Mater. Interfaces* **2016**, *8* (12), 8050−8057.

(38) Hsiao, S.-T.; Ma, C.-C. M.; Tien, H.-W.; Liao, W.-H.; Wang, Y.-S.; Li, S.-M.; Huang, Y.-C. Using a non-covalent modification to prepare a high electromagnetic interference shielding performance graphene nanosheet/water-borne polyurethane composite. *Carbon* **2013**, *60*, 57−66.

(39) Wu, Y.; Wang, Z.; Liu, X.; Shen, X.; Zheng, Q.; Xue, Q.; Kim, J.-K. Ultralight graphene foam/conductive polymer composites for exceptional electromagnetic interference shielding. *ACS Appl. Mater. Interfaces* **2017**, *9* (10), 9059−9069.

(40) Zhang, H.-B.; Yan, Q.; Zheng, W.-G.; He, Z.; Yu, Z.-Z. Tough graphene- polymer microcellular foams for electromagnetic interference shielding. *ACS Appl. Mater. Interfaces* **2011**, *3* (3), 918−924.

(41) Zhang, H.-B.; Zheng, W.-G.; Yan, Q.; Jiang, Z.-G.; Yu, Z.-Z. The effect of surface chemistry of graphene on rheological and electrical properties of polymethylmethacrylate composites. *Carbon* **2012**, *50* (14), 5117−5125.

(42) Li, C.; Yang, G.; Deng, H.; Wang, K.; Zhang, Q.; Chen, F.; Fu, Q. The preparation and properties of polystyrene/functionalized graphene nanocomposite foams using supercritical carbon dioxide. *Polym. Int.* **2013**, *62* (7), 1077−1084.

(43) Yan, D. X.; Pang, H.; Li, B.; Vajtai, R.; Xu, L.; Ren, P. G.; Wang, J. H.; Li, Z. M. Structured reduced graphene oxide/polymer composites for ultra-efficient electromagnetic interference shielding. *Adv. Funct. Mater.* **2015**, *25* (4), 559−566.

(44) Liang, C.; Qiu, H.; Han, Y.; Gu, H.; Song, P.; Wang, L.; Kong, J.; Cao, D.; Gu, J. Superior electromagnetic interference shielding 3D graphene nanoplatelets/reduced graphene oxide foam/epoxy nanocomposites with high thermal conductivity. *Journal of Materials Chemistry C* **2019**, *7* (9), 2725−2733.

(45) Chen, Z.; Xu, C.; Ma, C.; Ren, W.; Cheng, H. M. Lightweight and flexible graphene foam composites for high-performance electromagnetic interference shielding. *Advanced materials* **2013**, *25* (9), 1296−1300.

(46) Li, Y.; Pei, X.; Shen, B.; Zhai, W.; Zhang, L.; Zheng, W. Polyimide/graphene composite foam sheets with ultrahigh thermostability for electromagnetic interference shielding. *Rsc Advances* **2015**, *5* (31), 24342−24351.

(47) Yan, D.-X.; Pang, H.; Xu, L.; Bao, Y.; Ren, P.-G.; Lei, J.; Li, Z.-M. Electromagnetic interference shielding of segregated polymer composite with an ultralow loading of in situ thermally reduced graphene oxide. *Nanotechnology* **2014**, *25* (14), 145705.

(48) Tian, K.; Wang, H.; Su, Z.; He, J.; Tian, X.; Huang, W.; Guo, Y. Few-layer graphene sheets/poly (vinylidene fluoride) composites prepared by a water vapor induced phase separation method. *Materials Research Express* **2017**, *4* (4), 045603.

(49) Yan, D.-X.; Ren, P.-G.; Pang, H.; Fu, Q.; Yang, M.-B.; Li, Z.-M. Efficient electromagnetic interference shielding of lightweight graphene/polystyrene composite. *J. Mater. Chem.* **2012**, *22* (36), 18772−18774.

(50) Joseph, J.; Koroth, A. K.; John, D. A.; Sidpara, A. M.; Paul, J. Highly filled multilayer thermoplastic/graphene conducting composite structures with high strength and thermal stability for electromagnetic interference shielding applications. *J. Appl. Polym. Sci.* **2019**, *136* (29), 47792.

(51) Gupta, A.; Varshney, S.; Goyal, A.; Sambyal, P.; Gupta, B. K.; Dhawan, S. Enhanced electromagnetic shielding behaviour of multi-layer graphene anchored luminescent TiO2 in PPY matrix. *Mater. Lett.* **2015**, *158*, 167−169.

(52) Sambyal, P.; Dhawan, S.; Gairola, P.; Chauhan, S. S.; Gairola, S. Synergistic effect of polypyrrole/BST/RGO/Fe3O4 composite for enhanced microwave absorption and EMI shielding in X-Band. *Curr. Appl. Phys.* **2018**, *18* (5), 611−618.

(53) Mohan, R. R.; Varma, S. J.; Faisal, M.; S, J. Polyaniline/graphene hybrid film as an effective broadband electromagnetic shield. *RSC Adv.* **2015**, *5* (8), 5917−5923.

(54) Basavaraja, C.; Kim, W. J.; Kim, Y. D.; Huh, D. S. Synthesis of polyaniline-gold/graphene oxide composite and microwave absorption characteristics of the composite films. *Mater. Lett.* **2011**, *65* (19−20), 3120−3123.

(55) Li, Y.; Shen, B.; Yi, D.; Zhang, L.; Zhai, W.; Wei, X.; Zheng, W. The influence of gradient and sandwich configurations on the electromagnetic interference shielding performance of multilayered thermoplastic polyurethane/graphene composite foams. *Compos. Sci. Technol.* **2017**, *138*, 209−216.

(56) Chen, Y.; Wang, Y.; Zhang, H.-B.; Li, X.; Gui, C.-X.; Yu, Z.-Z. Enhanced electromagnetic interference shielding efficiency of polystyrene/graphene composites with magnetic Fe3O4 nanoparticles. *Carbon* **2015**, *82*, 67−76.

(57) Wan, Y.-J.; Yu, S.-H.; Yang, W.-H.; Zhu, P.-L.; Sun, R.; Wong, C.-P.; Liao, W.-H. Tuneable cellular-structured 3D graphene aerogel and its effect on electromagnetic interference shielding performance and mechanical properties of epoxy composites. *RSC Adv.* **2016**, *6* (61), 56589−56598.

(58) Lee, S.-H.; Kang, D.; Oh, I.-K. Multilayered graphene-carbon nanotube-iron oxide three-dimensional heterostructure for flexible electromagnetic interference shielding film. *Carbon* **2017**, *111*, 248−257.

(59) Yu, K.; Zeng, Y.; Wang, G.; Luo, X.; Li, T.; Zhao, J.; Qian, K.; Park, C. B. rGO/Fe 3 O 4 hybrid induced ultra-efficient EMI shielding performance of phenolic-based carbon foam. *RSC Adv.* **2019**, *9* (36), 20643−20651. Xia, Y.; Fang, J.; Li, P.; Zhang, B.; Yao, H.; Chen, J.;

Ding, J.; Ouyang, J. Solution-processed highly superparamagnetic and conductive PEDOT: PSS/Fe3O4 nanocomposite films with high transparency and high mechanical flexibility. *ACS Appl. Mater. Interfaces* **2017**, *9* (22), 19001–19010.

(60) Yadav, R. S.; Kuřitka, I.; Vilcakova, J.; Machovsky, M.; Skoda, D.; Urbănek, P.; Masař, M.; Jurča, M.; Urbánek, M.; Kalina, L.; Havlica, J. NiFe2O4 nanoparticles synthesized by dextrin from corn-mediated sol-gel combustion method and its polypropylene nanocomposites engineered with reduced graphene oxide for the reduction of electromagnetic pollution. *ACS omega* **2019**, *4* (26), 22069–22081.

(61) Pan, H.; Yin, X.; Xue, J.; Cheng, L.; Zhang, L. Microstructures and EMI shielding properties of composite ceramics reinforced with carbon nanowires and nanowires-nanotubes hybrid. *Ceram. Int.* **2017**, *43* (15), 12221–12231.

(62) Ru, J.; Fan, Y.; Zhou, W.; Zhou, Z.; Wang, T.; Liu, R.; Yang, J.; Lu, X.; Wang, J.; Ji, C.; et al. Electrically conductive and mechanically strong graphene/mullite ceramic composites for high-performance electromagnetic interference shielding. *ACS Appl. Mater. Interfaces* **2018**, *10* (45), 39245–39256. Ul Hassan, R.; Shahzad, F.; Abbas, N.; Hussain, S. Ceramic based multi walled carbon nanotubes composites for highly efficient electromagnetic interference shielding. *Journal of Materials Science: Materials in Electronics* **2019**, *30* (14), 13381–13388. Khan, N. T. Variation of electrical characteristics of EMI shielding materials coated with ceramic microspheres. *International Journal of Scientific Engineering and Technology* **2012**, *1* (5), 185–188.

(63) Qing, Y.; Su, J.; Wen, Q.; Luo, F.; Zhu, D.; Zhou, W. Enhanced dielectric and electromagnetic interference shielding properties of FeSiAl/Al2O3 ceramics by plasma spraying. *J. Alloys Compd.* **2015**, *651*, 259–265.

(64) Tan, Y.; Luo, H.; Zhou, X.; Peng, S.; Zhang, H. Dependences of microstructure on electromagnetic interference shielding properties of nano-layered Ti3AlC2 ceramics. *Sci. Rep.* **2018**, *8* (1), 7935.

(65) Xue, J.; Yin, X.; Ye, F.; Zhang, L.; Cheng, L. Theoretical prediction and experimental verification on EMI shielding effectiveness of dielectric composites using complex permittivity. *Ceram. Int.* **2017**, *43* (18), 16736–16743.

(66) He, P.; Cao, M.-S.; Cai, Y.-Z.; Shu, J.-C.; Cao, W.-Q.; Yuan, J. Self-assembling flexible 2D carbide MXene film with tunable integrated electron migration and group relaxation toward energy storage and green EMI shielding. *Carbon* **2020**, *157*, 80–89.

(67) Qing, Y.; Ma, L.; Hu, X.; Luo, F.; Zhou, W. NiFe2O4 nanoparticles filled BaTiO3 ceramics for high-performance electromagnetic interference shielding applications. *Ceram. Int.* **2018**, *44* (7), 8706–8709.

(68) Yuchang, Q.; Qinlong, W.; Fa, L.; Wancheng, Z.; Dongmei, Z. Graphene nanosheets/BaTiO 3 ceramics as highly efficient electromagnetic interference shielding materials in the X-band. *Journal of Materials Chemistry C* **2016**, *4* (2), 371–375. Ismail, M. M.; Rafeeq, S. N.; Sulaiman, J.; Mandal, A. Electromagnetic interference shielding and microwave absorption properties of cobalt ferrite CoFe2O4/polyaniline composite. *Appl. Phys. A: Mater. Sci. Process.* **2018**, *124* (5), 380. Sreedeviamma Dijith, K.; Vijayan, S.; Prabhakaran, K.; Peethambharan Surendran, K. Conducting La0.5Sr0.5CoO3-δ foams for harsh condition microwave shielding. *Journal of Industrial and Engineering Chemistry* **2019**, *78*, 330–337. Li, Q.; Yin, X.; Duan, W.; Kong, L.; Liu, X.; Cheng, L.; Zhang, L. Improved dielectric and electromagnetic interference shielding properties of ferrocene-modified polycarbosilane derived SiC/C composite ceramics. *Journal of the European Ceramic Society* **2014**, *34* (10), 2187–2201.

(69) Han, D.; Mei, H.; Xiao, S.; Cheng, L. Electromagnetic shielding properties of carbon-rich chemical vapor infiltration-prone silicon carbide matrix composites. *J. Am. Ceram. Soc.* **2018**, *101* (5), 1991–1998.

(70) Zhou, W.; Yin, R.-m.; Long, L.; Luo, H.; Hu, W.-d.; Ding, Y.-h.; Li, Y. SiC nanofibers modified Si3N4 ceramics for improved electromagnetic interference shielding in X-band. *Ceram. Int.* **2018**, *44* (2), 2249–2254.

(71) Bian, R.; He, G.; Zhi, W.; Xiang, S.; Wang, T.; Cai, D. Ultralight MXene-based aerogels with high electromagnetic interference shielding performance. *Journal of Materials Chemistry C* **2019**, *7* (3), 474–478.

(72) Wu, X.; Han, B.; Zhang, H.-B.; Xie, X.; Tu, T.; Zhang, Y.; Dai, Y.; Yang, R.; Yu, Z.-Z. Compressible, durable and conductive poly-dimethylsiloxane-coated MXene foams for high-performance electromagnetic interference shielding. *Chemical Engineering Journal* **2020**, *381*, 122622.

(73) Wang, Q. W.; Zhang, H. B.; Liu, J.; Zhao, S.; Xie, X.; Liu, L.; Yang, R.; Koratkar, N.; Yu, Z. Z. Multifunctional and water-resistant MXene-decorated polyester textiles with outstanding electromagnetic interference shielding and joule heating performances. *Adv. Funct. Mater.* **2019**, *29* (7), 1806819.

(74) Rojas, J.; Ribeiro, B.; Rezende, M. Influence of serrated edge and rectangular strips of MWCNT buckypaper on the electromagnetic properties of glass fiber/epoxy resin composites. *Carbon* **2020**, *160*, 317–327.

(75) Zhai, J.; Cui, C.; Ren, E.; Zhou, M.; Guo, R.; Xiao, H.; Li, A.; Jiang, S.; Qin, W. Facile synthesis of nickel/reduced graphene oxide-coated glass fabric for highly efficient electromagnetic interference shielding. *Journal of Materials Science: Materials in Electronics* **2020**, *31* (11), 8910–8922.

(76) Yang, J.; Liao, X.; Wang, G.; Chen, J.; Guo, F.; Tang, W.; Wang, W.; Yan, Z.; Li, G. Gradient structure design of lightweight and flexible silicone rubber nanocomposite foam for efficient electromagnetic interference shielding. *Chemical Engineering Journal* **2020**, *390*, 124589.

(77) Zhang, H.; Guo, Y.; Zhang, X.; Wang, X.; Wang, H.; Shi, C.; He, F. Enhanced shielding performance of layered carbon fiber composites filled with carbonyl iron and carbon nanotubes in the koch curve fractal method. *Molecules* **2020**, *25* (4), 969.

(78) Muthusamy, S.; Chung, D. Carbon-Fiber Cement-Based Materials for Electromagnetic Shielding. *ACI Mater. J.* **2010**, *107* (6), 602.

(79) Micheli, D.; Vricella, A.; Pastore, R.; Delfini, A.; Morles, R. B.; Marchetti, M.; Santoni, F.; Bastianelli, L.; Moglie, F.; Primiani, V. M.; et al. Electromagnetic properties of carbon nanotube reinforced concrete composites for frequency selective shielding structures. *Construction and Building Materials* **2017**, *131*, 267–277.

(80) Huang, S. W.; Chen, G. H.; Luo, Q.; Xu, Y. H. Electromagnetic shielding effectiveness of carbon black-carbon fiber cement based materials. *Advanced Materials Research* **2010**, *168*, 1438–1442.

(81) Cao, J.; Chung, D. Coke powder as an admixture in cement for electromagnetic interference shielding. *Carbon* **2003**, *41*, 2433–2436.

(82) Cao, J.; Chung, D. Use of fly ash as an admixture for electromagnetic interference shielding. *Cem. Concr. Res.* **2004**, *34* (10), 1889–1892.

(83) Wen, S.; Chung, D. Electromagnetic interference shielding reaching 70 dB in steel fiber cement. *Cem. Concr. Res.* **2004**, *34* (2), 329–332.

(84) Hosseini, E.; Arjmand, M.; Sundararaj, U.; Karan, K. Filler-free conducting polymers as a new class of transparent electromagnetic interference shields. *ACS Appl. Mater. Interfaces* **2020**, *12* (25), 28596–28606.

(85) Hong, X.; Chung, D. Carbon nanofiber mats for electromagnetic interference shielding. *Carbon* **2017**, *111*, 529–537. Kumar, V.; Muflikhun, M. A.; Yokozeki, T. Improved environmental stability, electrical and EMI shielding properties of vapor-grown carbon fiber-filled polyaniline-based nanocomposite. *Polym. Eng. Sci.* **2019**, *59* (5), 956–963.

(86) Shakir, H.; Tariq, A.; Afzal, A.; Abdul Rashid, I. Mechanical, thermal and EMI shielding study of electrically conductive polymeric hybrid nano-composites. *Journal of Materials Science: Materials in Electronics* **2019**, *30* (18), 17382–17392. Zhang, Y.; Pan, T.; Yang, Z. Flexible polyethylene terephthalate/polyaniline composite paper with bending durability and effective electromagnetic shielding performance. *Chemical Engineering Journal* **2020**, *389*, 124433.

(87) Fu, X.; Chung, D. Radio-wave-reflecting concrete for lateral guidance in automatic highways. *Cem. Concr. Res.* **1998**, *28* (6), 795–801.

(88) Guan, H.; Xie, J.; Chen, G.; Wang, Y. Facile synthesis of α-MnO2 nanorods at low temperature and their microwave absorption properties. *Mater. Chem. Phys.* **2014**, *143* (3), 1061−1068.

(89) Lee, T.-W.; Lee, S.-E.; Jeong, Y. G. Carbon nanotube/cellulose papers with high performance in electric heating and electromagnetic interference shielding. *Compos. Sci. Technol.* **2016**, *131*, 77−87.

(90) Xu, Y.; Zhang, D.; Cai, J.; Yuan, L.; Zhang, W. Effects of multi-walled carbon nanotubes on the electromagnetic absorbing characteristics of composites filled with carbonyl iron particles. *Journal of Materials Science & Technology* **2012**, *28* (1), 34−40.

(91) Geetha, S.; Kumar, K. K. S.; Meenakshi, S.; Vijayan, M. T.; Trivedi, D. C. Synergetic effect of conducting polymer composites reinforced E-glass fabric for the control of electromagnetic radiations. *Composites science and technology* **2010**, *70* (6), 1017−1022. Jang, J.-u.; Cha, J. E.; Lee, S. H.; Kim, J.; Yang, B.; Kim, S. Y.; Kim, S. H. Enhanced electrical and electromagnetic interference shielding properties of uniformly dispersed carbon nanotubes filled composite films via solvent-free process using ring-opening polymerization of cyclic butylene terephthalate. *Polymer* **2020**, *186*, 122030. Jin, X.; Ni, Q.-Q.; Natsuki, T. Composites of multi-walled carbon nanotubes and shape memory polyurethane for electromagnetic interference shielding. *J. Compos. Mater.* **2011**, *45* (24), 2547−2554. Sharif, M.; Ping, C. S.; Leong, K. Y. Electromagnetic interference shielding performances of MWCNT in concrete composites. *Solid State Phenomena* **2017**, *266*, 283−286.

(92) Joseph, N.; Sebastian, M. T. Electromagnetic interference shielding nature of PVDF-carbonyl iron composites. *Mater. Lett.* **2013**, *90*, 64−67.

(93) Yu, W.-C.; Xu, J.-Z.; Wang, Z.-G.; Huang, Y.-F.; Yin, H.-M.; Xu, L.; Chen, Y.-W.; Yan, D.-X.; Li, Z.-M. Constructing highly oriented segregated structure towards high-strength carbon nanotube/ultrahigh-molecular-weight polyethylene composites for electromagnetic inter-ference shielding. *Composites Part A: Applied Science and Manufacturing* **2018**, *110*, 237−245.

(94) Zeng, Z.; Zhang, Y.; Ma, X. Y. D.; Shahabadi, S. I. S.; Che, B.; Wang, P.; Lu, X. Biomass-based honeycomb-like architectures for preparation of robust carbon foams with high electromagnetic interference shielding performance. *Carbon* **2018**, *140*, 227−236.

(95) Gong, S.; Ni, H.; Jiang, L.; Cheng, Q. Learning from nature: constructing high performance graphene-based nanocomposites. *Mater. Today* **2017**, *20* (4), 210−219. Kuang, T.; Chang, L.; Chen, F.; Sheng, Y.; Fu, D.; Peng, X. Facile preparation of lightweight high-strength biodegradable polymer/multi-walled carbon nanotubes nano-composite foams for electromagnetic interference shielding. *Carbon* **2016**, *105*, 305−313. Wegst, U. G.; Bai, H.; Saiz, E.; Tomsia, A. P.; Ritchie, R. O. Bioinspired structural materials. *Nature materials* **2015**, *14* (1), 23−36. Xu, J.; Li, Y.; Hua, W.; Zhang, A.; Bao, J. Light-weight silver plating foam and carbon nanotube hybridized epoxy composite foams with exceptional conductivity and electromagnetic shielding property. *ACS Appl. Mater. Interfaces* **2016**, *8* (36), 24131−24142. Yang, J.; Liao, X.; Li, J.; He, G.; Zhang, Y.; Tang, W.; Wang, G.; Li, G. Light-weight and flexible silicone rubber/MWCNTs/Fe3O4 nano-composite foams for efficient electromagnetic interference shielding and microwave absorption. *Compos. Sci. Technol.* **2019**, *181*, 107670. Yao, Y.; Jin, S.; Ma, X.; Yu, R.; Zou, H.; Wang, H.; Lv, X.; Shu, Q. Graphene-containing flexible polyurethane porous composites with improved electromagnetic shielding and flame retardancy. *Compos. Sci. Technol.* **2020**, *200*, 108457.

(96) Kumar, P.; Shahzad, F.; Hong, S. M.; Koo, C. M. A flexible sandwich graphene/silver nanowires/graphene thin film for high-performance electromagnetic interference shielding. *RSC Adv.* **2016**, *6* (103), 101283−101287. Wang, Z.; Mao, B.; Wang, Q.; Yu, J.; Dai, J.; Song, R.; Pu, Z.; He, D.; Wu, Z.; Mu, S. Ultrahigh conductive copper/large flake size graphene heterostructure thin-film with remarkable electromagnetic interference shielding effectiveness. *Small* **2018**, *14* (20), 1704332.

(97) Hu, G.; Wu, C.; Wang, Q.; Dong, F.; Xiong, Y. Ultrathin nanocomposite films with asymmetric gradient alternating multilayer structures exhibit superhigh electromagnetic interference shielding

performances and robust mechanical properties. *Chemical Engineering Journal* **2022**, *447*, 137537.

(98) Liang, C.; Song, P.; Qiu, H.; Huangfu, Y.; Lu, Y.; Wang, L.; Kong, J.; Gu, J. Superior electromagnetic interference shielding performances of epoxy composites by introducing highly aligned reduced graphene oxide films. *Composites Part A: Applied Science and Manufacturing* **2019**, *124*, 105512.

(99) Harris, K. J.; Bugnet, M.; Naguib, M.; Barsoum, M. W.; Goward, G. R. Direct measurement of surface termination groups and their connectivity in the 2D MXene V2CT x using NMR spectroscopy. *J. Phys. Chem. C* **2015**, *119* (24), 13713−13720. Liu, J.; Liu, Z.; Zhang, H. B.; Chen, W.; Zhao, Z.; Wang, Q. W.; Yu, Z. Z. Ultrastrong and highly conductive MXene-based films for high-performance electromagnetic interference shielding. *Advanced Electronic Materials* **2020**, *6* (1), 1901094.

(100) Li, Y.; Tian, X.; Gao, S.-P.; Jing, L.; Li, K.; Yang, H.; Fu, F.; Lee, J. Y.; Guo, Y.-X.; Ho, J. S.; Chen, P.-Y. Reversible crumpling of 2D titanium carbide (MXene) nanocoatings for stretchable electro-magnetic shielding and wearable wireless communication. *Adv. Funct. Mater.* **2020**, *30* (5), 1907451.

(101) Weng, C.; Wang, G.; Dai, Z.; Pei, Y.; Liu, L.; Zhang, Z. Buckled AgNW/MXene hybrid hierarchical sponges for high-performance electromagnetic interference shielding. *Nanoscale* **2019**, *11* (47), 22804−22812.

(102) Xie, F.; Jia, F.; Zhuo, L.; Lu, Z.; Si, L.; Huang, J.; Zhang, M.; Ma, Q. Ultrathin MXene/aramid nanofiber composite paper with excellent mechanical properties for efficient electromagnetic interference shielding. *Nanoscale* **2019**, *11* (48), 23382−23391.

(103) Xin, W.; Xi, G.-Q.; Cao, W.-T.; Ma, C.; Liu, T.; Ma, M.-G.; Bian, J. Lightweight and flexible MXene/CNF/silver composite membranes with a brick-like structure and high-performance electromagnetic-interference shielding. *RSC Adv.* **2019**, *9* (51), 29636−29644.

(104) Wang, L.; Qiu, H.; Song, P.; Zhang, Y.; Lu, Y.; Liang, C.; Kong, J.; Chen, L.; Gu, J. 3D Ti3C2Tx MXene/C hybrid foam/epoxy nanocomposites with superior electromagnetic interference shielding performances and robust mechanical properties. *Composites Part A: Applied Science and Manufacturing* **2019**, *123*, 293−300.

(105) Han, M.; Shuck, C. E.; Rakhmanov, R.; Parchment, D.; Anasori, B.; Koo, C. M.; Friedman, G.; Gogotsi, Y. Beyond Ti3C2T x: MXenes for electromagnetic interference shielding. *ACS Nano* **2020**, *14* (4), 5008−5016.

(106) Jia, X.; Shen, B.; Chen, Z.; Zhang, L.; Zheng, W. High-performance carbonized waste corrugated boards reinforced with epoxy coating as lightweight structured electromagnetic shields. *ACS Sustainable Chem. Eng.* **2019**, *7* (22), 18718−18725.

(107) Ma, X.; Shen, B.; Zhang, L.; Chen, Z.; Liu, Y.; Zhai, W.; Zheng, W. Novel straw-derived carbon materials for electromagnetic interference shielding: a waste-to-wealth and sustainable initiative. *ACS Sustainable Chem. Eng.* **2019**, *7* (10), 9663−9670.

(108) Hou, Y.; Cheng, L.; Zhang, Y.; Du, X.; Zhao, Y.; Yang, Z. High temperature electromagnetic interference shielding of lightweight and flexible ZrC/SiC nanofiber mats. *Chemical Engineering Journal* **2021**, *404*, 126521.

(109) Mu, Y.; Zhou, W.; Wan, F.; Ding, D.; Hu, Y.; Luo, F. High-temperature dielectric and electromagnetic interference shielding properties of SiCf/SiC composites using Ti3SiC2 as inert filler. *Composites Part A: Applied Science and Manufacturing* **2015**, *77*, 195−203.

(110) Liang, C.; Hamidinejad, M.; Ma, L.; Wang, Z.; Park, C. B. Lightweight and flexible graphene/SiC-nanowires/poly (vinylidene fluoride) composites for electromagnetic interference shielding and thermal management. *Carbon* **2020**, *156*, 58−66.

(111) Mei, H.; Zhao, X.; Gui, X.; Lu, D.; Han, D.; Xiao, S.; Cheng, L. SiC encapsulated Fe@ CNT ultra-high absorptive shielding material for high temperature resistant EMI shielding. *Ceram. Int.* **2019**, *45* (14), 17144−17151.

(112) Han, G.; Ma, Z.; Zhou, B.; He, C.; Wang, B.; Feng, Y.; Ma, J.; Sun, L.; Liu, C. Cellulose-based Ni-decorated graphene magnetic film

for electromagnetic interference shielding. *J. Colloid Interface Sci.* **2021**, *583*, 571−578.

(113) Li, S.; Li, W.; Nie, J.; Liu, D.; Sui, G. Synergistic effect of graphene nanoplate and carbonized loofah fiber on the electromagnetic shielding effectiveness of PEEK-based composites. *Carbon* **2019**, *143*, 154−161.

(114) Wang, J.; Yang, K.; Wang, H.; Li, H. A new strategy for high-performance electromagnetic interference shielding by designing a layered double-percolated structure in PS/PVDF/MXene composites. *Eur. Polym. J.* **2021**, *151*, 110450.

(115) Yin, X.; Li, H.; Han, L.; Meng, J.; Lu, J.; Zhang, L.; Li, W.; Fu, Q.; Li, K.; Song, Q. Lightweight and flexible 3D graphene microtubes membrane for high-efficiency electromagnetic-interference shielding. *Chemical Engineering Journal* **2020**, *387*, 124025.